S-AA-M-12

OMEGA
System Operations Manual
Volume I–System Description
Chapter 5: Optomechanical System

Table of Contents

Chapter 5
Optomechanical System

5.0 INTRODUCTION

The Optomechanical System is defined as the optics and optomechanical support hardware necessary to transport the laser beams through the system from the laser drivers to the target. This system consists of the following subsystems: major structures, beamsplitters, mirrors, polarization control optics, spatial filters, frequency converters, focusing lenses, and alignment sensors. The laser amplifiers are not included, but the frequency-conversion crystals (FCC's) are, even though they are nonlinear optical components. The major beamline diagnostic instruments are operationally part of the Optomechanical System but are described in Chap. 7 of this document. The major structures serve as the stable support interface between all of the optical hardware (i.e., mirror mounts, spatial filters, etc.) and the Laser or Target Bay floors.

5.1 SYSTEM DESIGN

Configuration and Optical Design

The configuration and optical design of the system was constrained primarily by two factors: the need to fit the upgraded laser into the existing building and the desire to reuse as much hardware as possible (spatial filters, in particular). The top-level requirements for the total energy and the number of beams dictated the amplifier staging (see Chap. 3) and the required beam splitting, respectively. Optical damage thresholds dictated the minimum beam diameter in each stage that in turn fixed the magnification between stages. From these baselines the system was designed to incorporate image relaying and polarization controls, manage "ghost" reflections, equalize path beam lengths, and provide an accessible and serviceable layout.

Once the system configuration was determined, error budgets were developed for energy, wavefront, alignment, and polarization. Each budget was then distributed among individual components to formulate requirements for their design. For example, the wavefront budget dictated that the wavefront error contributed by each optical component not exceed $\lambda/10$ @ 1054 nm. This value is relatively small because the disk amplifiers consume a major portion of the error budget. The pointing error in the system is driven by the requirement to point beams onto target with a precision of ~5% of the target radius. Given a minimum target radius of 300 μm and a 1.8-m-focal-length final lens, the total pointing error budget is 8.33 μrad. The distribution of this error affected the design of the alignment sensor packages, the optical mounts, and the various structures supporting the laser. It was this pointing error budget that necessitated the implementation of the epoxy/granite structures for the stage-F alignment sensor packages (ASP's), which act as the optical alignment references for the system.

The energy budget specified the fluences at various points in the system, thereby impacting the choice of substrate material, typically BK-7 or fused silica. The energy-balance constraints drove a requirement for identical beam sizes at all the FCC's, to match the intensity and hence the conversion efficiency. This requirement forced a tight specification (±0.5%) for the focal length of the spatial-filter lenses. All lenses of a given type were corrected during fabrication such that their focal lengths are matched to ±0.2%.

The polarization budget prescribed the contrast of the polarization required for efficient splitting and amplification. The requirements for balanced beam-to-beam frequency conversion dictated the need for Brewster-angle polarizers ahead of the FCC's to achieve contrast ≥500:1. These are required in spite of the (50:1) polarization contrast the Brewster-angle disk amplifiers provide at the end of the amplifier stages. The disk amplifiers provide a relative insensitivity to depolarization early in the system.

The resultant design is a system that fits into the existing building and maximizes the use of equipment from the 24-beam OMEGA. (Over 90% of the existing OMEGA spatial filters were used in the upgraded system.) The system includes path-length adjusters that can provide simultaneous arrival of beam pulses at the target to within ±3 ps. For particular experimental purposes, individual beams can be intentionally mistimed to ±5 ns with respect to $t = 0$. Mapping the ultraviolet (UV) beams to the spherical target chamber was performed to minimize the sensitivity to variations in performance of the individual amplifiers. This mapping uses two mirrors per beam, ensures that incident angles on the mirrors are less than 60°, maintains equal path lengths from the FCC's to the target, and fits within the existing space. The system can produce laser beams with sufficient energy, quality, and alignment accuracy to attain the ultimate goal of 1%–2% nonuniformity on target.

Optomechanical Design

Four key constraints drove the design of the optomechanical assemblies. The first was strain-free mounting of all optical components. The mounts generally consist of three-point, six degree-of-freedom, exact-constraint designs that prevent optical distortion due to tolerance buildup from mount manufacturing, assembly, and environmental effects. The second key constraint is the need for precision pointing and centering control of optical components. These include fixed mounts, manual drives, and motorized drives that typically have μinch and/or μradian accuracy and stability requirements. The third constraint is to provide an adjustment range adequate to center the laser beam within the clear aperture of each optic. The range must be sufficient to compensate for typical fabrication and structure-installation tolerances. Finally, all optical components must be packaged within the space allocated by the system configuration.

Optical System Description

The overall system configuration for OMEGA is shown in Fig. 5.1-1. Figure 5.1-2 depicts the system staging and beam sizes. An overview description of the optical system, starting at the laser drivers, is as follows:

- Three laser drivers are located in the driver line area of the Laser Bay. For historical reasons, these are referred to as the main, the SSD, and the backlighter drivers. In normal operation, either the main or the SSD driver is used to feed the three initial legs of the beamlines. When the backlighter driver is used, it is injected into one leg and the other two remain available for use with either the main or the SSD driver. The backlighter driver is typically used to provide a different pulse shape and/or delay down one of the three legs.

- The SSD/main driver selection is made by inserting or removing a mirror in the driver beam train. This mirror directs the selected beam through an additional amplifier and to the A-splitter via an overhead relay tube. The driver alignment is performed using the driver alignment sensor package (ASP) at the base of the periscope that feeds the relay. Driver injection alignment is done at the stage-A ASP in the A-splitter.

- The backlighter driver is injected directly into any one of the A-splitter legs by means of mirrors that are manually placed on and within the splitter structure. This operation blocks the normal path to the selected leg from the driver-to-A-split relay. Injection alignment of the backlighter driver is performed using the backlighter ASP.

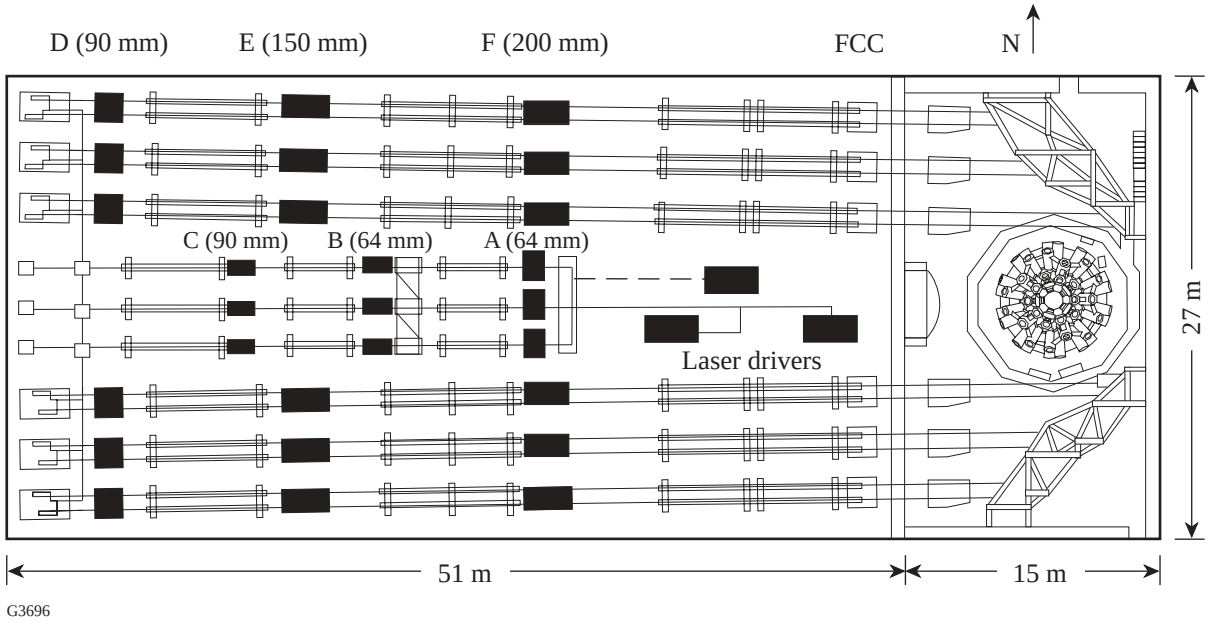

Figure 5.1-1
OMEGA system configuration: plan view.

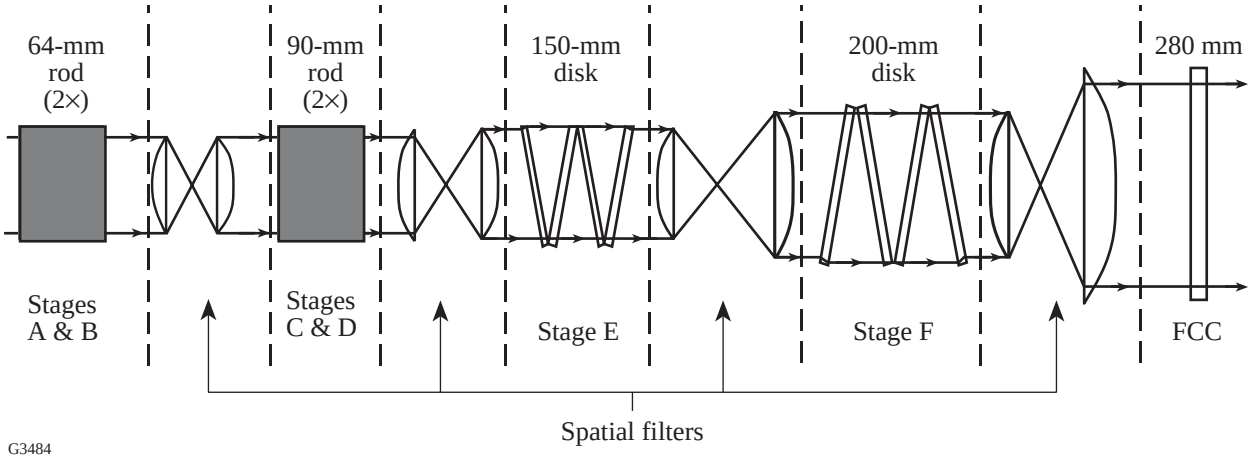

Figure 5.1-2
The amplifier staging of the OMEGA laser consists of four stages of rod amplifiers and two stages of disk amplifiers. The early stages compensate for the 1:60 splitting; the last three stages provide ~97% of the beamline energy.

- In normal operation, the driver-line beam enters the A-split structure, where it is split into three beams using a combination of polarizing beamsplitters, waveplates, and mirrors. Each of the three beams is then injected into a 64-mm-diam, stage-A amplifier. The path length in each of the legs through this first beam-splitting section is equal. Each stage-A amplifier is followed by a spatial filter that relays an image of the driver apodizer to the stage-B amplifier with a 1:1 magnification. (This is referred to as "imaging" the beam.)

- Each of the three beams enters a B beam-splitter structure, where it is split five ways vertically, making a total of 15 beams, each having equal energy. The path lengths are held nominally equal as the beams are directed into five-beam-high by one-beam-wide stage-B amplifier structures. The 64-mm stage-B amplifiers are followed by the stage-B spatial filters, which expand the beams to 86 mm. The input cells of the B spatial filters have variable spacers to adjust collimation of the legs.

- Each of these 15 beams then passes through the 90-mm stage-C amplifiers, stage-C spatial filters, stage-C polarizers (liquid crystal), and propagates to the stage-C relay structure. Each beam is then split into two beams, one directed north, the other south in the Laser Bay. Unity-magnification relays, identical to spatial filters but without the pinholes, are used to image the beams through this folding, to the stage-D splitting area, and on to the stage-D amplifiers. Path lengths are again kept nominally equal through the long paths to the stage-D beam-splitter structures. There are 30 beams at this point in the system.

- The C relays extend across the west end of the Laser Bay between the D-split structures and the D amplifiers. The relays are arranged on the structures to allow beams coming from legs 1, 2, and 3 to pass above and below the relay tubes; the same is true for beams folded into the D splits and going from the D splits to the D amplifiers. This is possible because legs 1, 2, and 3 are stepped upward relative to the floor in 6-in. increments from south to north. To accommodate these steps, clusters 2 and 5 are raised by 6 in. and clusters 1 and 4 by 12 in. These steps are illustrated in Fig. 1.3-3.

- Located at the end of each of the 15 legs is a C-ASP, which can view ≤1% of the beam through a "leaky" mirror located in the C-relay structure. The C-ASP's are used to monitor pointing and centering alignment for each of the legs.

- Beams exiting the C relays are folded into and enter the D-split structures, where each is again split horizontally into two beams and is folded in the path-length-adjustment system (PLAS). There are now 60 beams arranged in 6 clusters of 10 beams each, 5 high and 2 wide, with 30 beams returning eastward along each side of the Laser Bay. The PLAS assemblies, located within the stage-D beam-splitter structures, are two-mirror optical trombones. The mirror pairs in each beam can be individually positioned for precision control of the arrival time of the laser pulse at the target. The PLAS assemblies are used in combination with a beam-timing sensor in the target chamber to achieve a relative beam-timing accuracy of ≤3 ps at the target.

- Beams exiting the stage-D beam-splitter structure pass through and are amplified by the stage-D, 90-mm amplifier, then enter the stage-D spatial filters. The input cells of the D spatial filters have variable spacers to adjust collimation of the beamline. These spatial filters expand the beams for imaging into the 150-mm clear aperture, stage-E disk amplifiers. In addition, they are each positioned along the optical axis at the proper distance from the D amplifiers to compensate for the imaging differences caused by the ±20-cm path differentials in the various beamlines. After passing through

the stage-E amplifiers, the beams are expanded by a 1.33X stage-E spatial filter before entering the 200-mm, stage-F disk amplifier.

- The final, stage-F, amplifiers are followed by 1.4X stage-F spatial filters and the FCC's. The spatial filters bring the beams up to their final 280-mm clear aperture and relay the image just beyond the FCC's.

- The FCC's convert the high-power laser beams from 1054-nm to 351-nm wavelength, with up to 80% energy-conversion efficiency. Immediately before the FCC's, each beam is repolarized to ensure efficient frequency conversion to the UV.

- The frequency-converted beams then propagate through the shield wall to the F-ASP's located in the Target Bay. The primary pickoff in the ASP takes a 4% sample from each beam and focuses it into the F-ASP. During alignment, this sensor uses a three-mirror, off-axis telescope to produce a focal spot for pointing and centering alignment of both the 1054-nm and the 351-nm alignment beams. During a system shot, a partially reflective shutter directs 0.16% of the beam energy to the harmonic energy detector (HED), which measures the energy in all three harmonics: 1054 nm, 527 nm, and 351 nm.

- The remaining 96% of each high-power laser beam passes through the primary pickoff and is incident upon a distributed polarization rotator (DPR). The DPR's may be inserted or removed under computer-control. In conjunction with distributed phase plates (DPP's, described below) and smoothing by spectral dispersion (SSD, a feature of the driver line), DPR's serve to improve the uniformity of target irradiation. Each DPR has a color-dependent loss coefficient (approximately 1% in the blue, 2% in the green, and 6% in the red).

- Immediately following the DPR's are the stage-F calorimeters, which are used to calibrate the HED's. Also referred to as the "system calorimeters," each is a 12-in., full-aperture calorimeter that can measure energy with an accuracy of 1%. The calorimeters are flipped into the beams for system test shots or out for nominal target shots.

- Figure 5.1-3 illustrates the beam paths in the target area. The beams exiting the Laser Bay through the shield wall are in six clusters of ten beams and continue along the axis established in the Laser Bay until they reach their respective end mirrors. These mirrors, either 14-in. × 20-in. or 14-in. × 27-in. ellipses, are coated for high reflectance at 351 nm only. The residual red and green light (1054 nm and 532 nm) from the frequency-conversion process passes through the coating and the substrate to be diffused by an aluminum-oxide-coated plate behind the mirror. The end mirrors direct their respective beams to a target mirror mounted on the target mirror structure at a location chosen to best equalize the path length.

- The target mirrors, located on the ends of the hexagonal tubes of the target mirror structure (TMS), direct the beams through the hexagonal tubes to the focus lens assemblies (FLAS). The focus lenses are mounted on the target chamber and are centered on the line of sight between the target mirror center and the target (which is located in the center of the chamber). The focus lenses are 1.8-m-focal-length, single-element, *f*/6 aspheric lenses, with a 300-mm clear aperture. (The actual beam size is approximately 275 mm). Included in the FLAS assembly is a blast window assembly (BWA) that consists of a vacuum window and a debris shield. The high-power, 351-nm beams

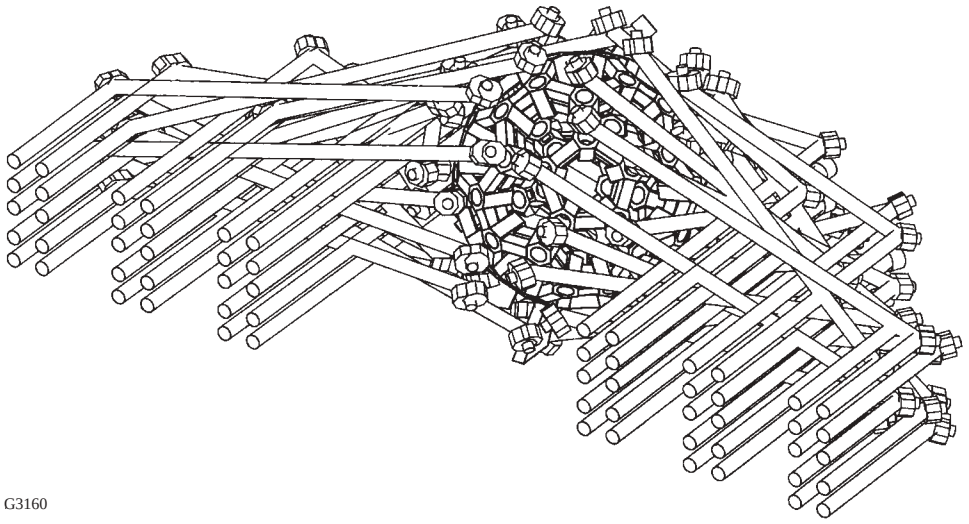

Figure 5.1-3
The beam paths of the OMEGA UV transport system. Each beamline has two mirrors: an end mirror and a target mirror. Care was taken in the design to ensure that all path lengths are nearly equal and the angle of incidence on all mirrors is <60°.

focus through these windows. The expendable debris shield is mounted on the output side of the vacuum window to protect it from being damaged by target fragments.

- The target is held in the center of the chamber by the target positioner and is aligned there by observing its position in two orthogonal directions with the target viewing system.

- An additional diffractive optic called a distributed phase plate (DPP) may be installed in each FLAS ahead of the focus lens itself. As mentioned earlier, these elements function in conjunction with the distributed polarization rotators (DPR's) and the smoothing by spectral dispersion (SSD) feature of the laser drivers to improve the uniformity of the target irradiation.

- Mounted on the Target Bay side of the shield wall, just ahead of the F-ASP's, are periscope mirror assemblies (PMA's). Each is used to inject a collimated, full-aperture, UV alignment beam into the UV beam path. The UV alignment table (UVAT) produces two alignment beams, one each for the north and south sides of the Target Bay. Each PMA is a motorized gantry system that can position a pair of mirrors on kinematic nests in any of the 30 beam paths on one side of the Target Bay to provide for injection of the UV alignment beam. Once the mirrors are in place on their kinematic nests, they can be actuated through the control system to co-align the UV alignment beam with the infrared (IR) alignment beam in the F-ASP.

5.2 MAJOR STRUCTURES

The major structures produced for OMEGA include 74 Laser Bay structures (23 unique designs) and 19 Target Bay structures (8 unique designs). These structures provide rigid and highly stable support

for the optomechanical assemblies and the laser amplifiers. This section gives a brief overview of the structural design approach, and several structures are described in detail. The key structural design requirements were

- accurately located mounting surfaces for the optical components and instruments,
- μinch and μradian stability within the facility's thermal and vibration environments, and
- packaging and servicing of the optical components and instruments within the constraints of the 60-beam configuration.

The typical approach used to mount and accurately position the optical components is as follows: (1) The structures are designed to be manufactured with critical mounting surfaces located to ±3 mm relative to surveyor pads provided on the structures. (2) The structures are surveyed into place to accuracies of ±3 mm. (3) Finally, the optical components have been designed to provide >±3-mm mounting adjustment and/or excess clear aperture. This adjustment range/excess clear aperture is adequate to compensate for the structure's fabrication and installation tolerances, thus ensuring that the optical system can be set up and aligned.

The requirements for pointing stability are among the most challenging. For reflective optics, allowable rotations of structural mounting surfaces are ±1.5 μrad, and for refractive optics, structural deflections must be within ~0.25 μm. These goals are met given the following environmental conditions: ±1°C temperature variations and vibration accelerations of up to 20 μg, with major peaks at 15 Hz, 20 Hz, and 30 Hz. The basic structural design approach uses massive steel space-frame structures grouted to the floor. Extensive finite-element analysis was used to confirm stability. The most complex example of this space-frame approach is the target mirror structure, which uses a 3-D "soccer ball" concept to accommodate OMEGA's 60 laser beams and provide the needed stiffness and mounting surfaces.

Laser Bay Structures

In the Laser Bay, the majority of the structures are box shaped, most about 3.6 m tall and either 0.9 or 1.8 m wide, and varying in length from ≤2 m to ≥10 m. The structures for the stage-B and C rod amplifiers and the B-splitters are box structures that are enclosed on three sides and the top with one side open for service access. The stage-D rod amplifiers are contained in 5-high × 2-wide structures, open on two sides for servicing (see Fig. 5.2-1). These structures are of a simple yet very rigid design that utilizes triangular sections. The spatial-filter structures (except the C relay) are box-beam space frames that rigidly support the filters in either 5-high × 1-wide or 5-high × 2-wide configurations. These open box-beam structures (see Fig. 5.2-2) are wide enough to allow for any spatial filter to be moved sideways out of the beamline during an alignment procedure if necessary.

The requirement to fit a 60-beam laser into the facility built for the original 24-beam OMEGA system made designing for serviceability more difficult. One of the greatest challenges involved servicing the disk amplifiers, which are 2 m long and weigh nearly 400 kg. Each amplifier has 32 high-voltage electrical cables, each about 13 mm thick, plus numerous cooling and nitrogen-purge lines attached. Since complete amplifiers must be replaced periodically, safety, reliability, and ease of operation were essential requirements of the design. The resulting structural design combines swinging doors and an overhead crane as integral parts for service and removal of the amplifiers (see Sec. 3.3 for more detail).

G5726

Figure 5.2-1
Stage-D amplifier structure.

G5727

Figure 5.2-2
Spatial filter structures are designed to allow each filter to be moved completely out of the beam for alignment.

Target Bay Structures

The design of the target area was dictated by the requirement to deliver 60 UV beams to the target chamber while providing access to the chamber for implementation of experimental devices. It is here where the design was most constrained by the existing building. The Target Bay structural layout, without the platform around the TMS, is shown in Fig. 5.2-3

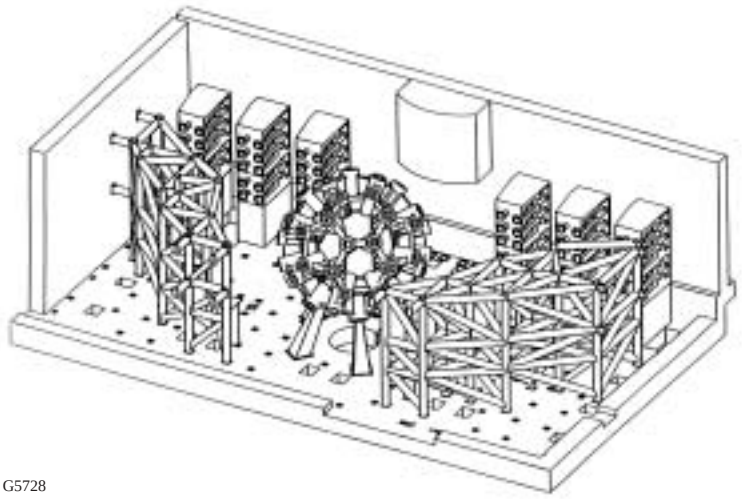

Figure 5.2-3
Target Bay structural configuration.

Laser beams, in six clusters of ten beams, come from the Laser Bay through 18-in.-diam holes in the shield wall. The beams first pass through the F-ASP structure, a notable exception to the space-frame approach used for all other structures. These unique structures serve as the pointing reference for the laser system and, as such, have exceptional stability requirements. The off-axis F-ASP optical system also contributed additional requirements that led to the unique mechanical design. The approach to this design was to "cast" a structure around the optical system space envelope using a structural epoxy composite, a material commonly used for machine-tool bases. This material and process provide a combination of high thermal and vibration damping with the ability to accurately mold critical off-axis optical mounting surfaces into the structure. The F-ASP is further described in Sec. 5.8.

After passing through the F-ASP's, the beams are incident upon the end mirrors, which are supported by two massive end mirror structures (EMS's). These 35-ton structures are constructed of 10-in. steel box beams, which support rigid interface plates for each end mirror. The basic functional requirements were to support the mirrors in a rigid and stable manner that did not obstruct the beam paths, and to provide for personnel access to the mirrors for servicing. Refer to Fig. 5.1-3 to see the mirror locations and the 60 beam paths.

Irradiation uniformity considerations led to the selection of an arrangement of beams on the target that is the same pattern as the gore stitching on a soccer ball: 20 hexagons and 12 pentagons with five-fold rotational symmetry about the vertical axis. The target mirror structure (TMS) (see Fig. 5.2-4) functions to position each of the final mirrors on the radial line that includes the port on the target chamber (TC) and target chamber center (where the targets are positioned). The TMS is also required to support a wide range of typically massive and bulky (but otherwise not well defined) target diagnostics while also allowing access to the ports on the TC itself.

G5729

Figure 5.2-4
The TMS has a soccer-ball geometry defined by the beam positions. The target chamber is supported and enclosed by the TMS. Each of the 60 beams enters the TMS through the radial hexagonal tubes. The 32 diagnostic ports are located in the hexagons and pentagons of the TMS.

The result is a steel structure made up of hexagonal tubes located at the vertices of the polygons and connected by wide I-beams that make the sides of the polygons. Modules consisting of several of the polygons were built as weldments. They were then assembled around the TC and bolted to form a complete, highly rigid, highly symmetrical structure. The TMS is supported from the Target Bay floor on six box-beam legs. The TC is supported by and within the TMS at six locations that correspond to the TMS legs.

The target mirrors (which do not appear in Fig. 5.2-3 or 5.2-4) are mounted on the outer ends of the hexagonal tubes at a radius of 3 m from the center of the TC. The mirrors are centered at a radius of 3.6 m and direct the beams radially inward through the hexagonal tubes toward the center of the TC.

Surrounding the TMS is a two-level personnel platform that provides access to the ports on the chamber, landing points for crane-hoisted material, and mounting points for ancillary diagnostic support systems (see Fig. 5.2-5). Key issues addressed in the design of the platform were potential interference with the many crossing laser beam paths and provision for room for the diagnostics, crane-load landing areas, work areas, and storage areas. All these had to be accommodated while maintaining safe access and egress for personnel. Note that the target mirror mounts are also shown in Fig. 5.2-5.

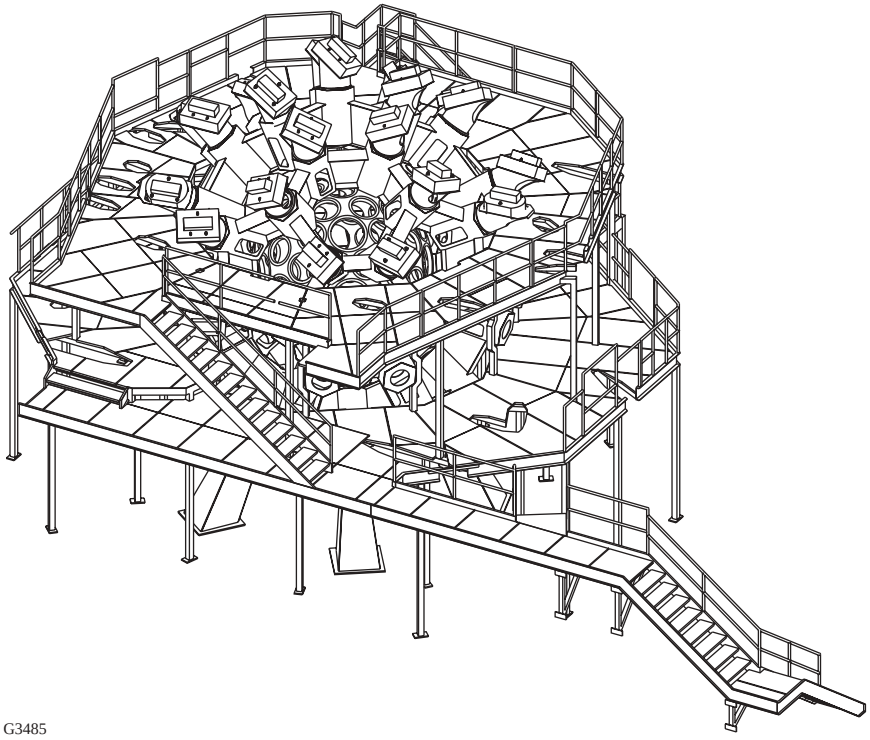

Figure 5.2-5
The personnel service platform for the TMS. The platform has two levels, is isolated from the TMS, and uses removable grids for flooring. The TMS is visible within the platform structure.

5.3 OPTICAL COMPONENTS

Optical components for OMEGA were procured through several major contracts with five leading optical fabrication vendors. This section summarizes the component specifications and their performance requirements.

The top-level requirements for the laser performance and uniformity dictated an array of lesser requirements for appropriate beam profiles and energy levels at the target while minimizing fluences throughout the laser system to reduce the chance of damage to optical components. From the requirements and configuration constraints, computer simulations of beam transport allowed determination of such parameters as fluence, *B*-integral, allowable wavefront and alignment error, and the required power balance.

Once the on-target error allowances were determined, optical engineers statistically apportioned the error among the components in the system. Budgets were made for the various types of error and used to establish surface finish and transmitted wavefront tolerances for each optical component. Once the fluences in the system were known, the optical material for each component could be chosen. The choice was typically between BK-7 for fluences below 2.0 J/cm^2 and fused silica for fluences above that.

Compilations of these parameters resulted in a specification control drawing (SCD) and statement of work (SOW) for each type of optical component in the OMEGA laser. Specifications were written for the following categories of optical components:

- Spatial-filter lenses
- Mirrors and beamsplitters
- Polarization control optics
- FCC's
- Aspheric focus lenses
- ASP optical components

Table 5.3-1 gives a listing of the system optical components (not including laser drivers); the typical specifications for these components (all measured at 1054 nm) are

Transmitted wavefront error:	±1/10 wave
Flatness (mirrors):	±1/20 wave
Surface roughness:	<10 Å (rms)

Optical Coatings

The requirements for OMEGA optical coatings are discussed in the Preliminary Design Document[1] and in detail in the Optics Coating Requirements Document.[2] The development of coatings, in general, and the UV transport mirror coating, in particular, are described in several reports in the LLE Review.[3,4] A coating specification[5] also outlines the required tests and inspection criteria for all coated optics. A summary of the coating requirements is given in Table 5.3-2. The coating designations in the left column of this table are discussed below.

The dielectric coatings for transport optics were produced in LLE's 54-in. and 72-in. vacuum coating chambers; the sol-gel coatings are produced in the Optical Manufacturing Facility at LLE by using dipping and spinning techniques. A great deal of effort also went into the design of the tooling for substrate cleaning and storage, coating tooling, testing tooling, and handling tooling to ensure that no process degrades the high-quality substrate surfaces. A substantial effort went into establishing a sol-gel coating capability for the 650 optics as well as a facility to clean the 2000 optics for OMEGA.

IR Coatings

The surfaces of the optics in the IR (1054 nm) portion of the laser system are coated with either anti-reflection (AR) or high reflection (HR) coatings, as appropriate.

The optics that have IR antireflection (1ωAR) coatings are either BK-7 glass or fused silica, depending on the incident fluence. The BK-7 substrates receive a vacuum-evaporated dielectric coating designs based on yttrium oxide/silicon dioxide or hafnium oxide/silicon dioxide. The fused silica spatial-filter input and output lenses receive a hafnium oxide/silicon dioxide (1ωAR) coating which provides a higher damage threshold. This hard oxide coating (HOCO) is preferred over a sol-gel coating for the spatial filter application because the sol-gel coatings can absorb oil contaminates from the spatial filter tube and the pumping system. Other fused silica optics on the system (i.e., LCP or LCW substrates and SSA windows) may be coated with a HOCO or a sol-gel coating. Although delicate to the touch, sol-gel has a very high damage threshold and is preferred at certain optic locations. The sol-gel coatings used on the disk amplifier windows receive an additional ammonia hardening step.

TABLE 5.3-1
OPTICAL COMPONENT SPECIFICATIONS

Part Number	Component Name	Qty.	Material	Width (mm)	Length/Diam. (mm)	Thick. (mm)	Coating Process	S1	S2	Scratch/Dig	C. A. (mm)	S1 PV 1054 nm	S1 RMS 1054 nm	S1 Grad 1054 nm	S1/S2 Å rms	S2/Trans PV 1054 nm	S2/Trans RMS 1054 nm	Gradient 1054 nm	Wedge
A-AB-C-75/A	20 cm SSA Windows	120	FS7940		228.6	10	H Sol-Gel	SG1ωAR	SG1ωAR	20/10H	215								
A-AC-C-45/A	15 cm SSA Windows	120	FS7940		177.8	10	H Sol-Gel	SG1ωAR	SG1ωAR	20/10H	165								
B-BN-C-02 Rev B	4.5 × 6 Beamsplitter	15	BK7	114.3	152.4	26	Dielectric	1ωRSTP45	1ωAR45	10/5	113	0.05	0.014	0.01	10	Trans 0.1	0.029	0.033	
B-BN-C-02 Rev B	4.5 × 6 "S" Leaky Mirror	1	BK7	114.3	152.4	26	Dielectric	1ω99RS45	1ωAR45	10/5	113	0.05	0.014	0.01	10	Trans 0.1	0.029	0.033	
B-BN-C-04 Rev B	5.5 × 7.5 Beamsplitter	45	BK7	139.7	190.5	19.6	Dielectric	1ωRSTP45	1ωAR45	20/10	145	0.05	0.014	0.01	10	Trans 0.1	0.029	0.033	
B-BN-C-04 Rev B	5.5 × 7.5 "P" Leaky Mirror	15	BK7	139.7	190.5	19.6	Dielectric	1ω99RP45	1ωAR45	20/10	145	0.05	0.014	0.01	10	Trans 0.1	0.029	0.033	
B-BM-C-01 Rev B	4.5 × 6 Mirror	50	Pyrex	114.3	152.4	26	Dielectric	1ωHR45	Stress comp	10/5	108	0.05	0.014	0.01	10	S2 10	—	—	
B-BM-C-02 Rev B	5.5 × 7.5 Mirror	220	Pyrex	139.7	190.5	32.3	Dielectric	1ωHR45	Stress comp	20/10	143	0.05	0.014	0.01	10	S2 10	—	—	
B-BM-C-03 Rev A	6 × 9 Mirror	20	Pyrex	152.4	228.6	38.6	Dielectric	1ωHR45	Stress comp	20/10	155	0.05	0.014	0.01	10	S2 10	—	—	
B-BM-C-12-1	14" × 27" × 2" Trans Mirror	40	Pyrex	355.6	685.8	50.8	Dielectric	3ωHR		20/10		0.1	0.028	0.01	10	—	—	—	—
B-BM-C-12-2	14" × 27" × 3" Trans Mirror	20	Pyrex	355.6	685.8	76.2	Dielectric	3ωHR		20/10		0.1	0.028	0.01	10	—	—	—	—
B-BM-C-13	14" × 20" × 2" Trans Mirror	60	Pyrex	355.6	508	50.8	Dielectric	3ωHR		20/10		0.1	0.028	0.01	10	—	—	—	—
B-BP-C-01-1 Rev B	Stage A–D LC Substrate QWP	60	BK7		135	15.2	Dielectric	LC6.5	1ωAR	10/5	115	0.05	0.013	0.017	10	Trans 0.1	0.029	0.033	2 Sec.
B-BP-C-01-1 Rev B	Stage A–D LC Substrate HWP	30	BK7		135	15.2	Dielectric	2LC6.5	1ωAR	10/5	115	0.05	0.013	0.017	10	Trans 0.1	0.029	0.033	2 Sec.
B-BP-C-01-2 Rev B	Stage A–D LC Substrate QWP	15	FS7940		135	15.2	Sol-Gel or Dielectric	LC6.5	SG or 1ωAR	10/5	115	0.05	0.013	0.017	10	Trans 0.1	0.029	0.033	2 Sec.
B-BP-C-01-2 Rev B	Stage E LC Substrate QWP	60	BK7		200	25.9	Dielectric	LC6.5	1ωAR	30/10	180	0.05	0.013	0.017	10	Trans 0.1	0.029	0.033	2 Sec.
B-BP-C-03 Rev B	FCC Polaizer	60	BK7	337	603	25.4	Dielectric	Pol/1ω	None	30/10		—	—	—	10	Trans 0.1	0.029	0.033	2 Sec.
B-BP-C-04-1 Rev B	Stage A–D LC Pol	96	BK7		135	15.2	Dielectric	LC9	1ωAR	10/5	115	0.125	0.033	0.033	10	Trans 0.1	0.029	0.033	30 Sec.
B-BP-C-04-2 Rev B	Stage A–D LC Pol	15	FS7940		135	15.2	Sol-Gel or Dielectric	LC9	SG or 1ωAR	10/5	115	0.125	0.033	0.033	10	Trans 0.1	0.029	0.033	30 Sec.
B-BP-C-05 Rev B	Stage E LC Pol	60	BK7		200	25.9	Dielectric	LC9	1ωAR	30/10	180	0.125	0.033	0.033	10	Trans 0.1	0.029	0.033	30 Sec.
B-BS-C-01 Rev A	Stage A Spatial Filter Lens	6	FS7940		99.1	9.7	Dielectric	1ωAR	1ωAR	20/5	70	0.125	0.033	0.033	10	S2 0.125	0.033	0.033	
B-BS-C-11 Rev A	Stage B Spatial Filter Input Lens	15	FS7940		99.1	9.7	Dielectric	1ωAR	1ωAR	20/5	70	0.125	0.033	0.033	10	S2 0.125	0.033	0.033	
B-BS-C-10 Rev A	Stage B Spatial Filter Output Lens	15	BK7		149.4	12.7	Dielectric	1ωAR	1ωAR	20/5	100	0.125	0.033	0.033	10	S2 0.125	0.033	0.033	
B-BS-C-02 Rev A	Stage C Spatial Filter Lens	30	FS7940		149.4	12.7	Dielectric	1ωAR	1ωAR	20/5	100	0.125	0.033	0.033	10	S2 0.125	0.033	0.033	
B-BS-C-03 Rev A	Stage C Relay Lens	60	BK7		149.4	12.7	Dielectric	1ωAR	1ωAR	20/5	100	0.125	0.033	0.033	10	S2 0.125	0.033	0.033	
B-BS-C-04 Rev A	Stage D Spatial Filter Input Lens	60	FS7940		149.4	12.7	Dielectric	1ωAR	1ωAR	20/10	100	0.125	0.033	0.033	10	S2 0.125	0.033	0.033	
B-BS-C-05 Rev A	Stage D Spatial Filter Output Lens	60	BK7		213.5	20.2	Dielectric	1ωAR	1ωAR	20/10	170	0.125	0.033	0.033	10	S2 0.125	0.033	0.033	
B-BS-C-06 Rev A	Stage E Spatial Filter Input Lens	60	FS7940		213.5	20.2	Dielectric	1ωAR	1ωAR	20/10	170	0.125	0.033	0.033	10	S2 0.125	0.033	0.033	
B-BS-C-07 Rev A	Stage E Spatial Filter Output Lens	60	BK7		283.4	25.2	Dielectric	1ωAR	1ωAR	20/10	235	0.125	0.033	0.033	10	S2 0.125	0.033	0.033	
B-BS-C-08 Rev A	Stage F Spatial Filter Input Lens	60	FS7940		283.4	25.2	Dielectric	1ωAR	1ωAR	20/10	235	0.125	0.033	0.033	10	S2 0.125	0.033	0.033	
B-BS-C-09 Rev A	Stage F Spatial Filter Output Lens	60	BK7		372.3	35.2	Dielectric	1ωAR	1ωAR	30/10	320	0.125	0.033	0.033	10	S2 0.125	0.033	0.033	
B-BE-B-01 Rev D	Frequency Conversion Crystal	60	KDP		300	12	Sol-Gel	SG1ωAR	SG1/2ωAR	80/20	290	—	—	—	50	Trans 0.2	0.048	0.055	6 sec.
B-BE-B-01 Rev D	Frequency Conversion Crystal	60	KDP		300	12	Sol-Gel	SG1/2ωAR	SG3ωAR	80/20	290	—	—	—	50	Trans 0.2	0.048	0.055	6 sec.
B-BE-C-22-2	FCC UV Absorption Window	60	F11		300	10	Dielectric	1ωAR	3ωR50%	20/10	280	0.1	—	—	10	Trans 0.1	0.028	0.033	6 sec.
B-BE-C-H2 Rev C	Second Tripler Crystal	60	KDP		300	8	Sol-Gel	SG3ωAR	SG3ωAR	40/20H	284	—	—	—	50	Trans. 0.24	—	0.05	6 sec.
B-BE-C-G4 Rev D	Birefringent Wedge-DPR	60	KDP		300	10	Sol-Gel	SG3ωAR	SG3ωAR	40/20H	284	—	—	—	50	Trans. 0.24	—	0.05	4,5 sec.
B-BL-C-01	F/6 Aspheric Focus Lens	60	FS7940		325	22	Sol-Gel	SG3ωAR	SG3ωAR	30/10	300	—	—	—	10	Trans 0.083	0.024	0.024	
B-BL-C-04	Blastshield-Vacuum Window	60	FS7940		325	25.4	Sol-Gel	SG3ωAR	SG3ωAR	20/10	300	—	—	—	10	Trans 0.095	0.028	0.033	15 sec.
B-BL-C-05 Rev A	Distributed Phase Plate-DPP	60	FS7940		310	14	Sol-Gel	SG3ωAR	SG3ωAR	20/10H	290	0.1	0.03	0.033	10	S2/T 0.1	0.03	0.033	10 sec.
B-BL-C-07 Rev B	Debris Shield	60	FS7940		297	5	Sol-Gel	SG3ωAR	SG3ωAR	40/20H	280	—	—	—	10	Trans. 0.15	0.06	0.06	10 sec.
B-CB-C-06	Primary Pickoff Lens	60	FS7940		350	25.4	Sol-Gel	None	SG3ωAR	20/10	325	0.047	0.014	0.017	10	Trans 0.095	0.028	0.033	
B-CB-C-11 Rev D	HED Filter Input Window	60	FS7940		72.05	10.2	Note 1	None	None	20/10	40	1	0.333	0.333	10	T/S2 1	0.333	0.333	1°
B-CB-C-12	HED Filter Output Window	60	FS7940		72.05	10.2	Note 1	123ω AR	123ω AR	20/10	40	1	0.333	0.333	10	T/S2 1	0.333	0.333	
B-CB-C-B6 Rev A	Window HED Pickoff	60	FS7940	127	140	17.4		None	None	20/10	128 ×	0.333	0.083	0.111	10	Trans 0.333	0.083	0.111	20 min.
B-CB-C-4	Window, Shot Diag. Pickoff	60	NG-11		135	19.2		None	None	20/10		0.047	0.014	0.017	10	—	—	—	
B-CB-C-03	Mirror, Secondary, FASP	60	Zdur		101.6	13.2		AL/SiO_2		10/5	86.6	0.05	0.014	0.017	10	S2 10	—	—	
B-CB-C-02	Mirror, Tertiary, FASP	60	Zdur		101.6	13.2		AL/SiO_2		10/5	86.6	0.05	0.014	0.017	10	S2 10	—	—	
B-CB-C-01	Mirror, Final, FASP	60	Zdur		101.6	13.2		AL/SiO_2		10/5	90	0.05	0.014	0.017	10	S2 10	—	—	
			Note 1) 123 ω AR R < 0.5% @ 1 ω, 3 ω and R 4% at 2ω – Fluence = 0.01 of main beam fluence = .038 J/cm^2																

Table 5.3-2
OMEGA Coating Requirements

Coating Designation	LC Gap	Wavelength	Incident Angle	Control Value	Reflectance		Transmittance		Max. Fluence* (J/cm^2)
					S%	P%	P%	P/S	
1ωHRSP45		1054 nm	45°	R	99.5	>99.5			5.4
1ωRSTP45		1054 nm	45°	R	>99.5	<4.0	>96		5.4
1ω99RS45		1054 nm	45°	R	99±0.5				5.4
1ω99RP45		1054 nm	45°	R		99±0.5			4.5
1ωStressAR		1054 nm	45°	R	<1.0	<0.5			5.4
1ωAR		1054 nm	0	R	<0.5	<0.5			5.6
POL (1ωRSTP57)		1054 nm	57°	T			95	500/1	5.1
1ωAR45		1054 nm	45°	R	<1.0	<0.5			5.4
LCS6.5	6.5 μm	No Optical Requirements							
2 LCS6.5	13 μm								
LCS9	>18 μm								
1ωARALIGN		1054 nm	0°	R	<1.0	<1.0			2.9
		351 nm	0°	R	>10	>10			2.9
SG1/2ωAR		703 nm (cwl)	0°	R	<1.0	<1.0			2.9
SG1ωAR		1054 nm	0°	R	<0.5	<0.5			5.4
SG3ωAR		351 nm	0°–10°	R	<0.5	<0.5			2.9
3ωHRSP(ANG)		351 nm	0°–60°	R	>99.5	>99.5			2.9
1/2/3ωAR		351/527/1054	0	R	>85	>85			low power

cwl = center wavelength

*Note: Fluences assume 7-ns foot (F) pulse and 1.1-ns main (M) pulse.

HR coatings are applied to high reflectivity mirrors, partial reflectors, 45°-incidence polarizing beam splitters, and 57°-incidence polarizers. These coatings are based on a vacuum-evaporated dielectric coating design using tantalum oxide/silicon dioxide or hafnium oxide/silicon dioxide. These materials were developed for high damage threshold and optical performance. During initial manufacture of the 5.5-in. × 7.5-in. reflector coating, stresses from the coating process deformed the optic, causing the optics to fail optical surface-figure testing. After several remedies were investigated, the best solution was found to be a coating (1ωStressAR) that, when applied to the back side of the optics, produces similar stresses. This rear-side coating is applied to all mirror substrates coated with dielectric multilayers.

FCC Assembly Coatings

The FCC assembly converts the high-power, 1054-nm laser beam to 351 nm. The assembly contains a full-aperture IR linear polarizer, a UV absorption window before the crystals, and, finally, three potassium dihydrogen phosphate (KDP) FCC's. The IR polarizer is a dielectric coating operating at a 57° angle of incidence. The UV absorber has a dielectric AR @ 1054 nm (1ωAR) on S1 and dielectric 1ωAR that is also ~50% reflecting @ 351 nm on S_2. The coating for the FCC's is a two-layer design where the first layer applied is a moisture barrier coating of either a thermosetting polysiloxane (GR650) or a polymethylmethacrylate (PMMA) material and the final coating is the sol-gel. The coating designs are optimized for three wavelengths (SG1ωAR, SG1.5ωAR, and SG3ωAR) depending on the surface. These coatings are applied on the crystals using dipping and spinning deposition processes.

UV Optics

The UV (351-nm) transport optics are coated with a sol-gel antireflection coating (SG3ωAR) for the transmissive optics and a dielectric, high-reflector coating [3ωHRSP(ANG)] for the transport mirrors. For each dielectric application, the composition and design (using hafnium oxide/silicon dioxide) of the coatings vary depending on the incidence angle of the beam and the orientation of the electric vector with respect to the coated surface. For a given angle, each design provides the specified reflectance using the minimum number of layers to improve damage characteristics. These designs are also modified to reduce the time-averaged electric field in the upper layers of the coatings.

5.4 POLARIZATION MANAGEMENT

Proper management of the polarization at various stages of the OMEGA laser is crucial for achieving peak performance and good uniformity on target. Polarization control involves the elimination of the effects of birefringence (such as polarization rotation) in passive and active component materials and the minimization of phase retardation in coatings. Thermally induced stress birefringence in the laser amplifiers must not unduly restrict the shot-to-shot cycle time. In the design phase, a complete polarization control error budget was developed. Table 5.4-1 is a list of polarization management requirements and their respective design implementations. Figure 5.4-1 is a system schematic showing the location of the polarization control optics from the B amplifier to the FCC's, not including the splits.

Table 5.4-1
Polarization Management Plan

Polarization Requirement	Design Plan
• Driver-line isolation	• Thin-film plate polarizers and Faraday rotator
• Beam splitting for initial beam balance	• Polarizing beam splitters and LC wave plates
• Reset linear polarization for stage-C split	• LCP followed by 1/4 wave plate
• Circular polarization in rod amplifiers	• 1/4 wave plate and LCP after beam splitters
• Birefringence cleanup after rods	• LCP
• Set linear polarization for disk amplifiers	• LCP, followed by 1/4 wave plate
• Birefringence cleanup before FCC's	• 28-cm-clear-aperture linear plate polarizer
• Control phase retardation in UV mirrors	• Proper specs and deposition of coatings

Thin-Film Brewster-Angle Linear Polarizers

The OMEGA design utilizes thin-film Brewster-plate linear polarizers in the driver-line large-aperture ring amplifiers (LARA's) and isolators, and just before the frequency converters where the beam's clear aperture is 280 mm. Figure 5.4-2 illustrates the operation of a typical Brewster-angle polarizer: *p*-polarization is transmitted and *s*-polarization is reflected. The minimum contrast required in the driver isolators is 200:1, whereas the FCC polarizers are required to be ≥500:1. LLE coats high-quality polarizers with 70-mm clear apertures for the drivers and 280-mm clear apertures for the FCC's. These polarizers meet or exceed the contrast and damage thresholds for their respective locations in the system.

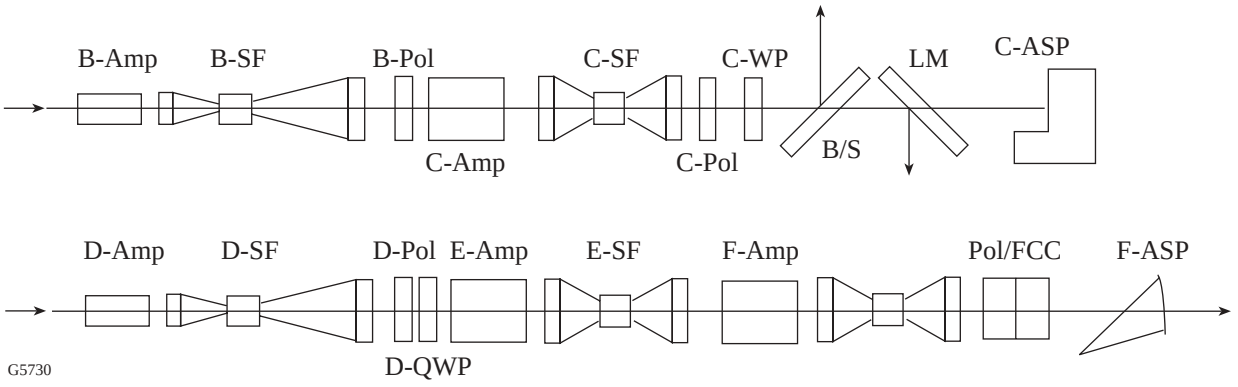

Figure 5.4-1
Laser system schematic showing location of polarization control optics in laser-amplifier stages.

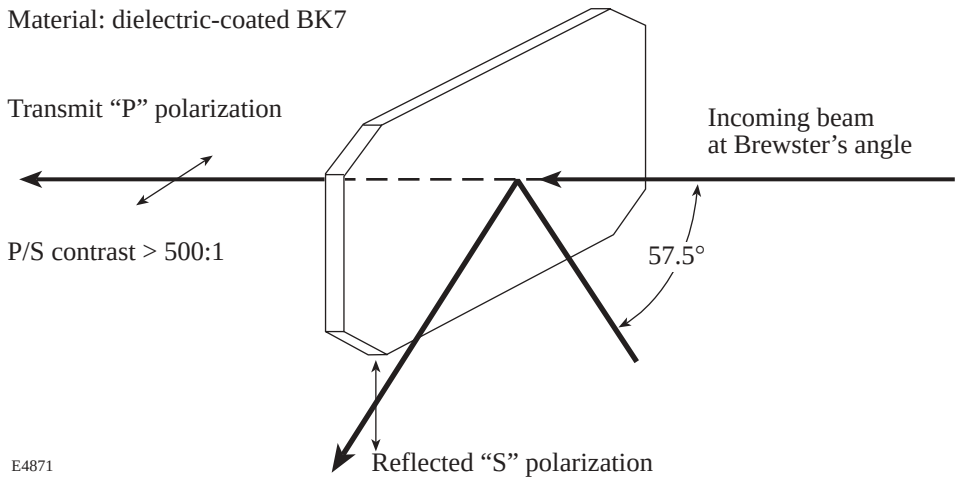

Figure 5.4-2
Schematic of Brewster-angle linear polarizers.

Thin-Film Polarizing Beam Splitters

All beam splitting in the OMEGA laser system uses a combination of liquid-crystal wave plates (LCW's) and thin-film polarizing beamsplitters designed to operate at 45°. The splitting ratio (see Fig. 5.4-3) is variable from 0.5 Rs to 0.99 Rs and is adjusted by rotating the preceding wave plate. Any ellipticity due to phase retardation that occurs in the splitting areas is eliminated with the liquid-crystal polarizers (LCP's) located ahead of the amplifiers. The wave plates are adjustable in rotation about the optical axis to achieve small corrections (±5%) in beam-splitting ratios for the purpose of beam-to-beam energy balance.

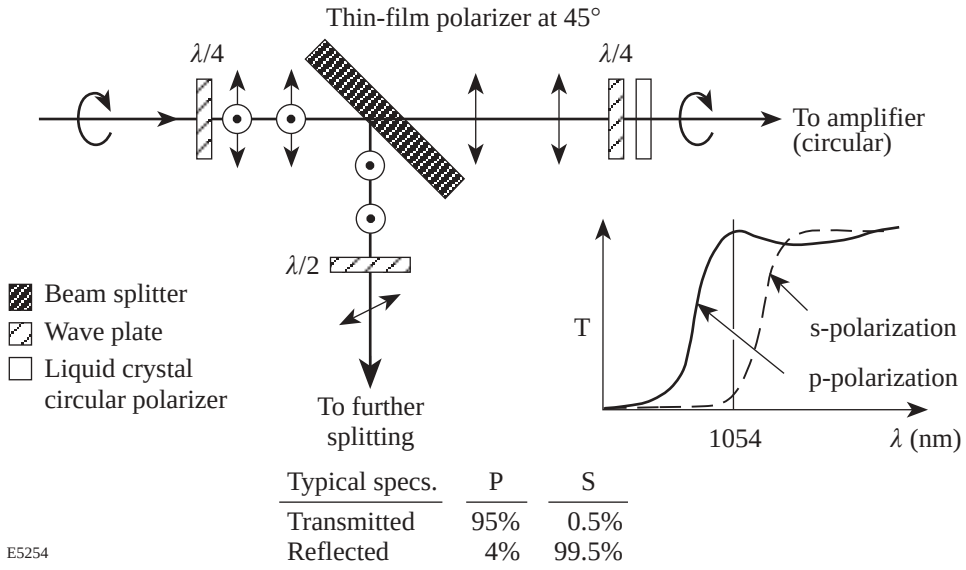

Figure 5.4-3
Polarizing 45° beamsplitter. This design allows for a variable split ratio of 20:1 to 1:1. The reflected and transmitted beams are orthogonally polarized. This arrangement permits adjustments to be made for beam balance without affecting beam polarization.

Liquid-Crystal Polarizers

The liquid-crystal polarizers (LCP's) are low-cost devices developed at LLE[6] for the purpose of improving the contrast in circularly polarized, 1054-nm laser beams. These pure circular polarizers are used before and after the 64-mm and 90-mm rod amplifiers for maintaining pure circularly polarized light in rod amplifiers and to ensure that linear polarization can be produced for the disk amplifiers. They are fabricated from two antireflection (AR)-coated, flat optical plates (BK7 or fused silica) with a thin layer (18 μm) of liquid-crystal fluid in between. Details of their design and performance are discussed in Sec. 8.3.2 of the OMEGA Upgrade Preliminary Design Document (Title I).[1] The largest (150-mm c.a.) LCP is located at the output of the stage-D spatial filter, just ahead of the stage-E disk amplifier.

Wave Plates

Liquid-crystal half- and quarter-wave plates operating at 1054 nm are required in 64-mm and 90-mm clear apertures for beam splitting and beam-balance control in the splitters of stages A, B, C, and D. Liquid-crystal quarter-wave (LCW) plates convert beams from linear to circular polarization and vice versa. The largest LCW is at the output of the stage-D spatial filter just prior to the stage-E disk amplifier. LLE has fabricated liquid-crystal quarter-wave plates for OMEGA in sizes up to 150-mm clear aperture (200-mm diam) (see Sec. 8.3.1 of the Title I document).

5.5 BEAM-SPLITTING SUBSYSTEMS

The four beam-splitting regions (A, B, C, and D) divide the incoming beam into three, five, two, and two equal-energy beams, respectively. Due to the nature of the components, however, the process is not 100% efficient. This loss is accounted for in the design of the system.

All beam splits are performed with 45°-angle-of-incidence, polarizing beam splitters. A polarizing beam splitter transmits the *p*-polarized part of the incident beam and reflects the *s*-polarized component. The split ratio is adjustable over a range of 0.05 R_s to 0.95 R_s by varying the amounts of *s*- and *p*-polarized light incident on the beam splitter using a wave plate (just ahead of the splitter) to rotate the polarization vector (see Fig. 5.4-3). A perfect beam splitter has 100% contrast in both the reflected and transmitted arms; that is, pure *s* is reflected and pure *p* is transmitted. The OMEGA polarizing beam splitters transmit the *p*-polarized component of the incident beam with >99% contrast; however, the reflected *s*-polarized component contains 4% of the *incident p*-polarized light. The beam-splitting and balancing process accounts for that imperfect contrast (even if it reaches much higher levels) by accepting a loss in the splitting regions. For the sake of accurate control of beam balance, no attempt is made to recover the lost energy.

A-Split

Figure 5.5-1(a) shows the components and beam paths in the A-split structure for the main and SSD Drivers. At the top of the structure, the 61-mm-diam, *s*-polarized beam from the driver relay enters and is directed by mirror M01 to beam combiner BS0. The 1054-nm, *p*-polarized alignment beam from the infrared alignment table (IRAT) comes into the lower part of the structure via mirror M05 and is injected via mirrors M04, M03, and M02 through the back of the same beam combiner BS0. After BS01, quarter-wave plate QW01 can be rotated to achieve circularly polarized light and maximize transmission of either the driver beam or the IRAT beam. Liquid-crystal polarizer LCP01 is fixed in rotation, but any light it transmits is pure circular polarization. It will attenuate the driver or IRAT beam if QW01 is rotated to produce elliptical polarization. From this point, beam splitting occurs as follows (Note: the component numbers used here are only for the purpose of describing the A-split. They are not the same as those used in the system-control database.):

- Quarter-wave plate QW02 converts the circularly polarized light from LCP01 to elliptically polarized light and is rotated to achieve 66:33% splitting at BS03, with 33% of the light passing through BS03 and going to Leg 3.

- *P*-polarized light transmitted through BS03 is directed to Leg 3 via M31, M32, M33 and is circularized by quarter-wave plate QW31; then LCP31 purifies the circular polarization. QW31 can be used to tune the balance of energy in Leg 3 if necessary.

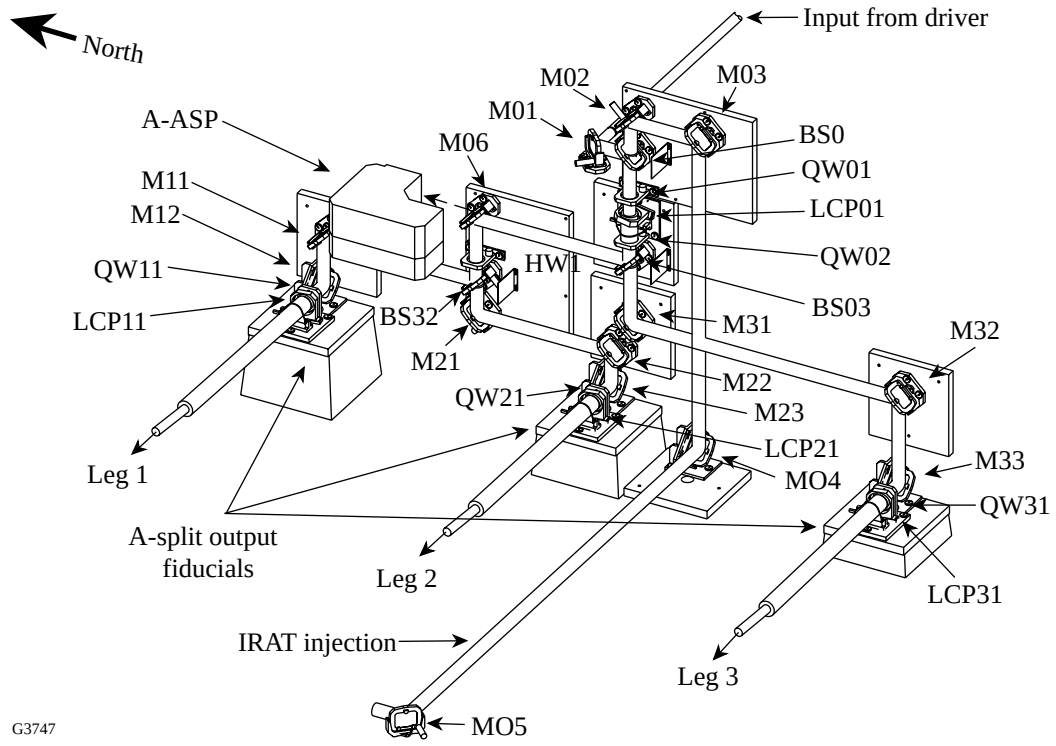

Figure 5.5-1(a)
Components and beam paths for the main and SSD drivers in the A-split structure. The A-split structure uses several beam splitters and wave plates to achieve equal splitting of the driver to Legs 1, 2, and 3.

- *S*-polarized light reflected from BS03 is directed to mirror M06, which reflects ≥98% downward toward beamsplitter BS32. The ≤2% light transmittted by M06 goes into the stage-A ASP, which is used for pointing and centering alignment of the driver and IRAT beams.

- The *s*-polarized light reflected by M06 passes through half-wave plate HW1, which adjusts the rotation of the linear polarization axis (to 45°) at beam splitter BS32 to achieve a 50%:50% split. Thus, 50% is *s*-polarized and reflects from BS32, and 50% is *p*-polarized and transmits through BS32.

- The *s*-polarized light from BS32 is directed into Leg 1 via mirrors M11 and M12. As in Leg 3, the quarter-wave plate QW11 converts the linear-polarized light to circular; LCP11 purifies the circular polarization; and the combination can be used to attenuate for beam balance.

- The *p*-polarized light transmitted by BS32 is directed to Leg 2 via mirrors M21, M22, and M23 and then passes through QW21 and LCP21 to become circularly polarized.

- The initial procedure to achieve precision beam balance among Legs 1, 2, and 3 is contained in the OMEGA Upgrade System Activation Plan (S-AA-M-10). After that, the control system is used to operate the motorized wave plates via the LON network in response to energy-balance measurements on the laser output.

- Figures 5.5-1(b)–5.5-1(d) show the components and beam paths that have been added in the A-splitter for the backlighter driver. The backlighter beam enters through a hole in the back of the A-split. This allows for simultaneous propagation of the backlighter and either the SSD or main driver.

  Each of the leg beams has an energy of about 1.5 J at the output of the A-splitter.

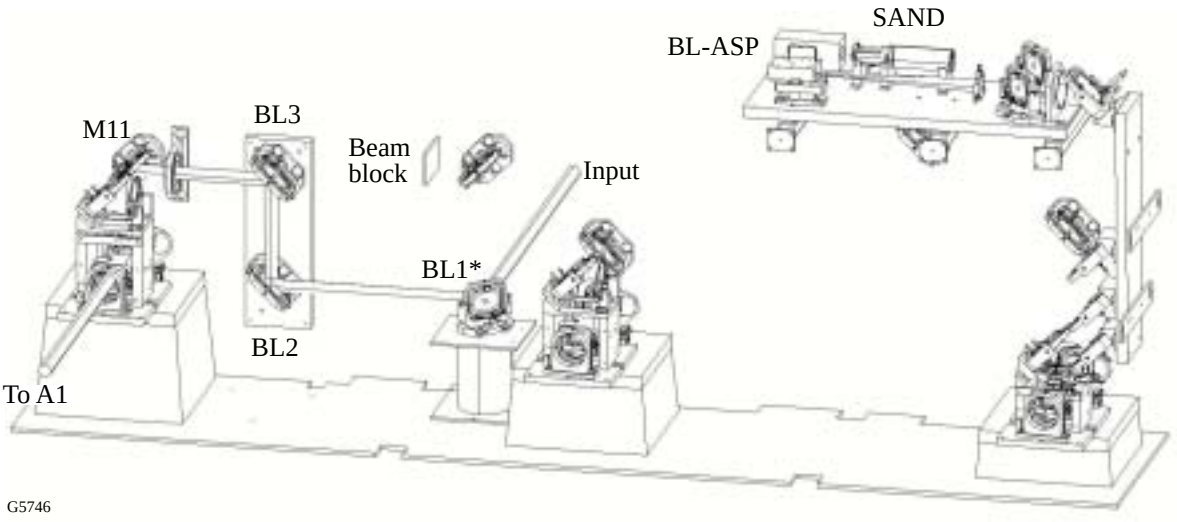

Figure 5.5-1(b)
Components and beam paths for the backlighter driver and backlighter-ASP configured for use in Leg 1 of the A-split structure.

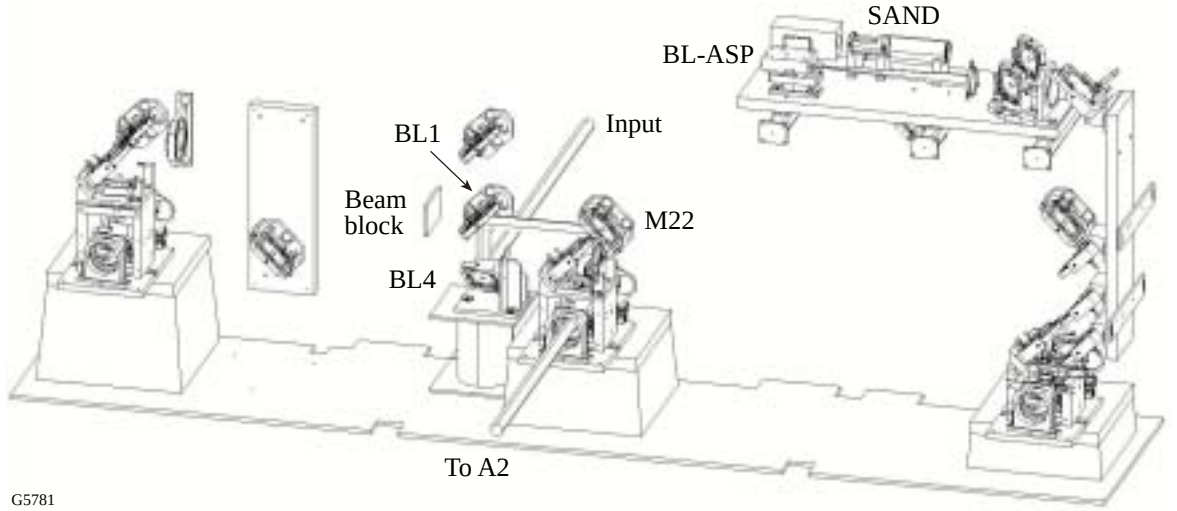

Figure 5.5-1(c)
Components and beam paths for the backlighter driver and backlighter-ASP configured for use in Leg 2 of the A-split structure.

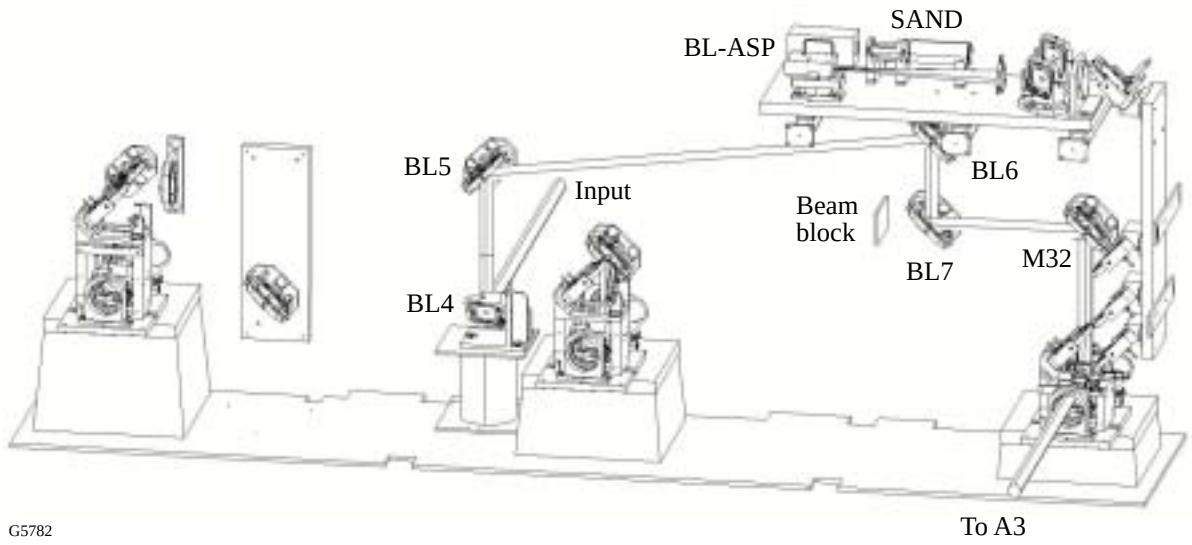

Figure 5.5-1(d)
Components and beam paths for the backlighter driver and backlighter-ASP configured for use in Leg 3 of the A-split structure.

B-Split

Each of the three stage-B beam-splitter arrays splits a stage-A output beam (~14 J) emerging from a 64-mm stage-A amplifier into five equal energy beams that are injected into the vertical array of stage-B 64-mm rod amplifiers. As a result of insertion and tuning losses, the energy per beam at the output of the splitter is about 2.5 J. The B-split array shown in Fig. 5.5-2 contains four beamsplitters, 13 HR45 mirrors, six quarter-wave LCW's, three half-wave LCW's, and six LCP's. The beam splitters are all variable-polarization beam splitters with splitting ratios adjustable over a range of 0.05 R_s to 0.95 R_s by tuning the preceding wave plate (therefore they are all capable of 50:50). The reflected and transmitted beams are always elliptically polarized and must be circularized after reflection or transmission with the wave plates.

The input beam, from the A amplifier, is circularly polarized; the first LCP cleans the circular polarization and rejects any birefringent light. The quarter-wave LCW prior to BS1 is used for precision tuning at BS1 to create a split ratio of 0.80R/0.20T. The transmitted beam from BS1 then reflects off four HR45 mirrors, is recircularized by a quarter-wave LCW, cleaned by an LCP, and then propagates to the B amplifier in Leg 15 as circularly polarized light. The LCW/LCP combination can be used for fine tuning by attenuation, if necessary. The reflected light from BS1 passes through a half-wave LCW prior to BS2, where its ellipticity is adjusted to achieve 0.25R/0.75T at BS2. The sequence of splitting and recircularizing each beam is similar in each of the five split beams (legs). The sequence of adjusting the ellipticity with half-wave LCW's prior to each splitter, to achieve the proper splitting ratio, is also similar for each of these splits. For each of the five output beams the split ratios multiply as follows:

Leg 11: $1.0 \times (0.8\text{R} \times 0.75\text{T} \times 0.67\text{T} \times 0.5\text{T}) = 0.2$
Leg 12: $1.0 \times (0.8\text{R} \times 0.75\text{T} \times 0.67\text{T} \times 0.5\text{R}) = 0.2$

Leg 13: $1.0 \times (0.8R \times 0.25R) = 0.2$
Leg 14: $1.0 \times (0.8R \times 0.75T \times 0.33R) = 0.2$
Leg 15: $1.0 \times 0.2T = 0.2$

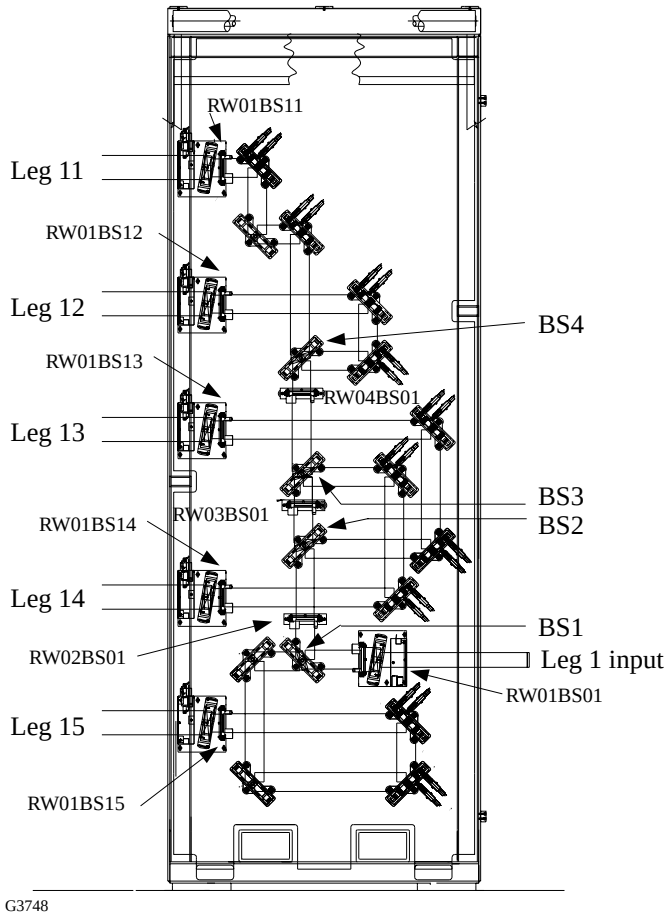

Figure 5.5-2
B-split structure showing the array of wave plates and beam splitters used to achieve the five-way split (Leg 1 is shown).

C-Split

The C-split area for each of the 15 legs exiting the stage-C spatial filters is a simple 50:50 split (see Fig. 5.5-3). The C-polarizer structure, following the C-spatial filter, contains an LCP that cleans the circularly polarized beam, followed by a quarter-wave LCW that converts the light to linear polarization. The polarization vector is oriented at 45° to achieve a 50:50 split at the beam splitter. The reflected beam from each splitter is directed to clusters 1, 2, and 3 on the north side of the Laser Bay. The transmitted beam is turned to the south toward clusters 4, 5, and 6 by a 0.98R "leaky" mirror. The 2% of the light that passes through the leaky mirror goes into the C-ASP for pointing and centering alignment. (The ASP is normally shuttered during high-energy shots.)

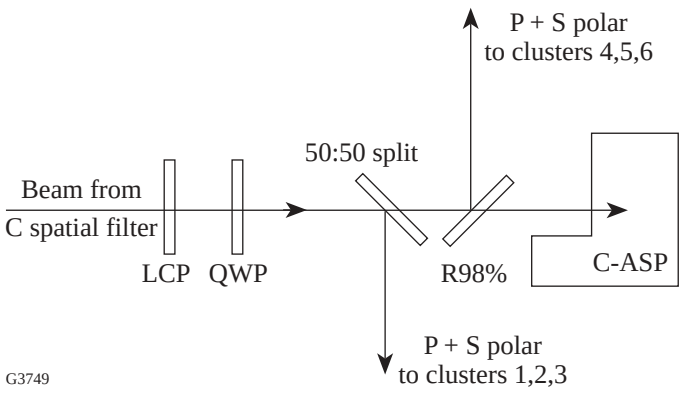

Figure 5.5-3
C-split area for each of the 15 beams from the ABC legs.

D-Split

The stage-D beamsplitting structures are located at the north and south corners of the west end of the Laser Bay. At each of the five levels of the stage-D beam-splitter structure, a single beam with either *p*- or *s*-polarization (*s*–north, *p*–south) is injected by the stage-D input mirror (see Fig. 5.5-4). The half-wave LCW at the input rotates the polarization vector to 45°, allowing for a 50:50 split. The resulting beams are folded and directed into PLAS's and are then pointed through the beamlines. At the entrance to the structure, each beam passes through a computer-controlled, rotatable half-wave LCW, which is used to control the split ratio. The fold mirrors and beam splitters are mounted in 5-in. × 7-in. gimbals and motorized where necessary for alignment control. The beams reflected from the fold mirrors travel into the two-mirror PLAS's; these are set to adjust for the incoming path differential, plus the residual of the path differential from the FCC's to target. The PLAS's have dc-motorized slides that are

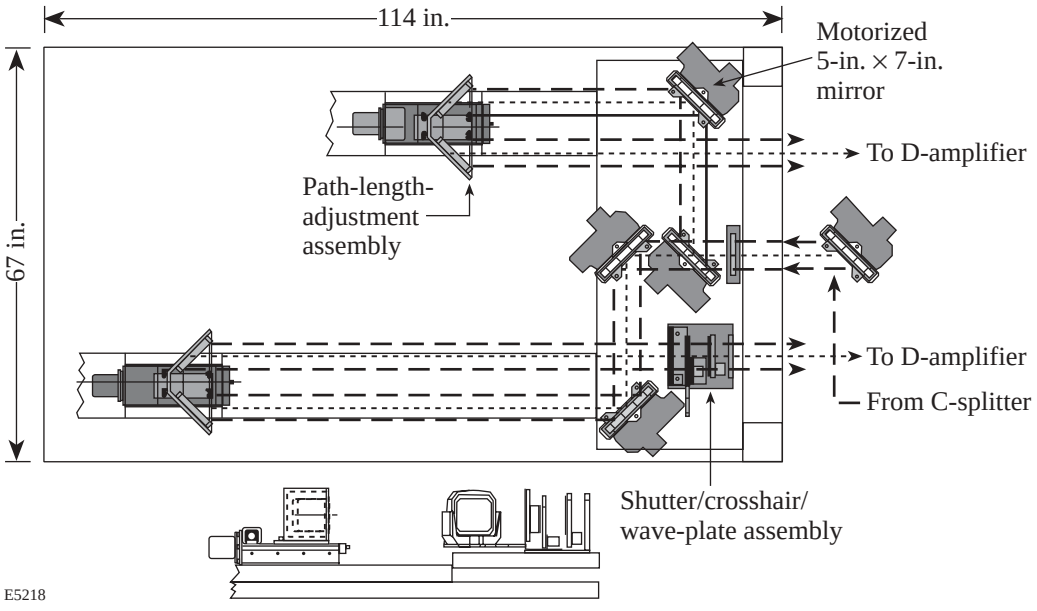

Figure 5.5-4
Stage-D beam-splitting configuration, showing path-length adjusters.

used for fine path-length adjustment or the deliberate mistiming required for some experiments and provide a range of travel approximately equal to ±5 ns. Following the PLAS, each beam has a shutter/cross-hair/wave-plate assembly. Each of these contains a computer-operated, pneumatically actuated shutter and cross hair; a computer-controlled, rotatable, quarter-wave LCW to circularly polarize the beam; and a LCP to enhance the polarization contrast prior to entry into the D amplifiers.

5.6 SPATIAL FILTERS

A total of 243 evacuated spatial filters and relays are used in stages A thru F. The elements of a typical spatial filter are shown in Fig. 5.6-1. Each filter consists of an evacuated stainless steel tube with a plano-convex lens at each end and a pinhole manipulator mounted in the middle. They provide spatial filtering, image relaying, and various amounts of magnification. The filter sizes depend on the beam aperture and magnification; for instance, the stage-A filter is *f*/50 and 5.6 m long, and the stage-F filter is *f*/22 and 10.25 m long. Table 5.6-1 shows the sizes and optical parameters of the spatial filters

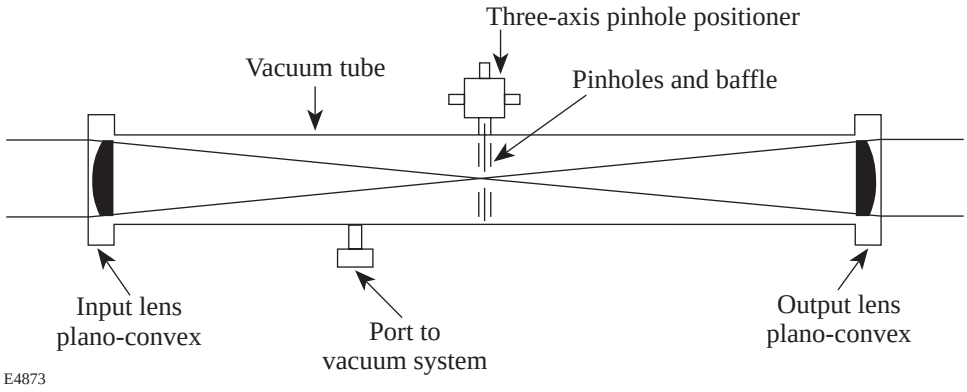

Figure 5.6-1
Schematic of an OMEGA spatial filter.

Table 5.6-1
Spatial Filter Parameters
(All dimensions in mm)

	Overall	Focal Length		Physical Aperture		Clear Aperture		Beam Size	
	Length	Input	Output	Input	Output	Input	Output	Input	Output
Driver-A	12548	6274	6274	76	76	70	70	56	56
Stage-A	5588	2794	2794	76	76	70	70	56	56
Stage-B	3757	1527	2230	76	123	70	100	56	82
Stage-C	6000	3000	3000	123	123	100	100	82	82
C Relay	6175	3088	3088	123	123	100	100	82	82
Stage-D	5904	2168	3737	123	185	100	170	82	141
Stage-E	7462	3198	4264	185	255	170	235	141	189
Stage-F	10234	4264	5970	255	348	235	320	189	264

and relays in stages A–F. Mildly aspheric lenses are used in all the large-aperture spatial filters to reduce the accumulated spherical error in the system. Focal lengths of the lenses are specified at ≤1% accuracy to meet mechanical tolerances for assembly. In addition, the focal lengths of lens pairs are matched to 0.5% accuracy in order to equalize the magnification of all filters in a given stage. This maintains the beam-to-beam magnification (i.e., matching of beam diameter at the FCC's) within the error budget for total-energy balance.

The spatial filters are built in five subsections: the tube weldments, the lens cells, the lens spacers, the interface package, and the pinhole manipulator. The tube weldments are 316-stainless-steel tubes with flanges and are rated for 5×10^{-6} Torr. The nominal operating pressure for the spatial filters is 2 mTorr. This pressure is maintained for all 243 filters using a centralized vacuum system that is described later in this section. Experiments have determined that a pressure at 5 mTorr is sufficient to avoid air breakdown or nonlinear optical effects in the focal region.

The lens cells and lens spacers are mounted on each end of the weldments. The cells are one-piece annular mounts for the lens and contain two O-ring grooves for vacuum seals, one on the spacer side and the other on the lens side. The plano-convex lenses are mounted in the cells with their plano sides against an O ring and facing the vacuum. Simple threaded rings or retainer clips are used to firmly hold the lenses centered in their mounts prior to evacuating the filters. The lens spacer is an annular aluminum cylinder used to compensate for variations in the focal length of the lenses and manufacturing tolerances of the tube weldments. Custom sizing of each spacer for a specific tube and lens pair allows the collimation of each spatial filter to be strictly maintained. The length of the spacers is determined to ≤125 μm using a special fixture and shearing interferomtric techniques, thereby providing collimation of each spatial filter to $\leq \lambda/4$ @ 1.054 nm. The exception to the fixed customized spacers are the variable spacers located on the stage-B and stage-D input spatial-filter tubes. These variable spacers are utilized to provide for collimation adjustments.

The pinhole manipulator provides adjustments in three orthogonal axes to allow the pinhole to be correctly positioned at the focal point of the spatial-filter input lens. Existing pinhole manipulators fitted with new dc motors are used for stages A–D. The size and space constraints of the stage-E and F spatial filters required fabrication of a new manipulator that has the slides and motors located within the spatial-filter tube. The mechanical and electrical components of these manipulators are vacuum compatible.

All of the spatial filters in stages B thru F (not the C relays) are mounted in structures that have sufficient platform space to allow the filters to be moved to one side of the beam path when necessary. To achieve this, the interface between the spatial filter and the support structure is an air bearing that when powered from the system nitrogen supply, allows the entire filter to be moved out of the beam.

Spatial-Filter Vacuum System

The 243 OMEGA system spatial filters are evacuated to 2 mTorr by a centralized spatial-filter vacuum system. The system has three Edwards GV600 dry vacuum pumps (connected together by a manifold) mounted on a vibration-isolated pad in the OMEGA facility fan room, located on the first floor, south of the Capacitor Bays. Figure 5.6-2 shows a schematic of the pumps and four-branch piping layout. The piping system, which runs under the Laser Bay floor, is built with 6-in. stainless steel welded tubing. All four branches are connected to a manifold system that allows any of the three pumps to evacuate the entire system. Pipes are run up to the Laser Bay through holes in the floor and

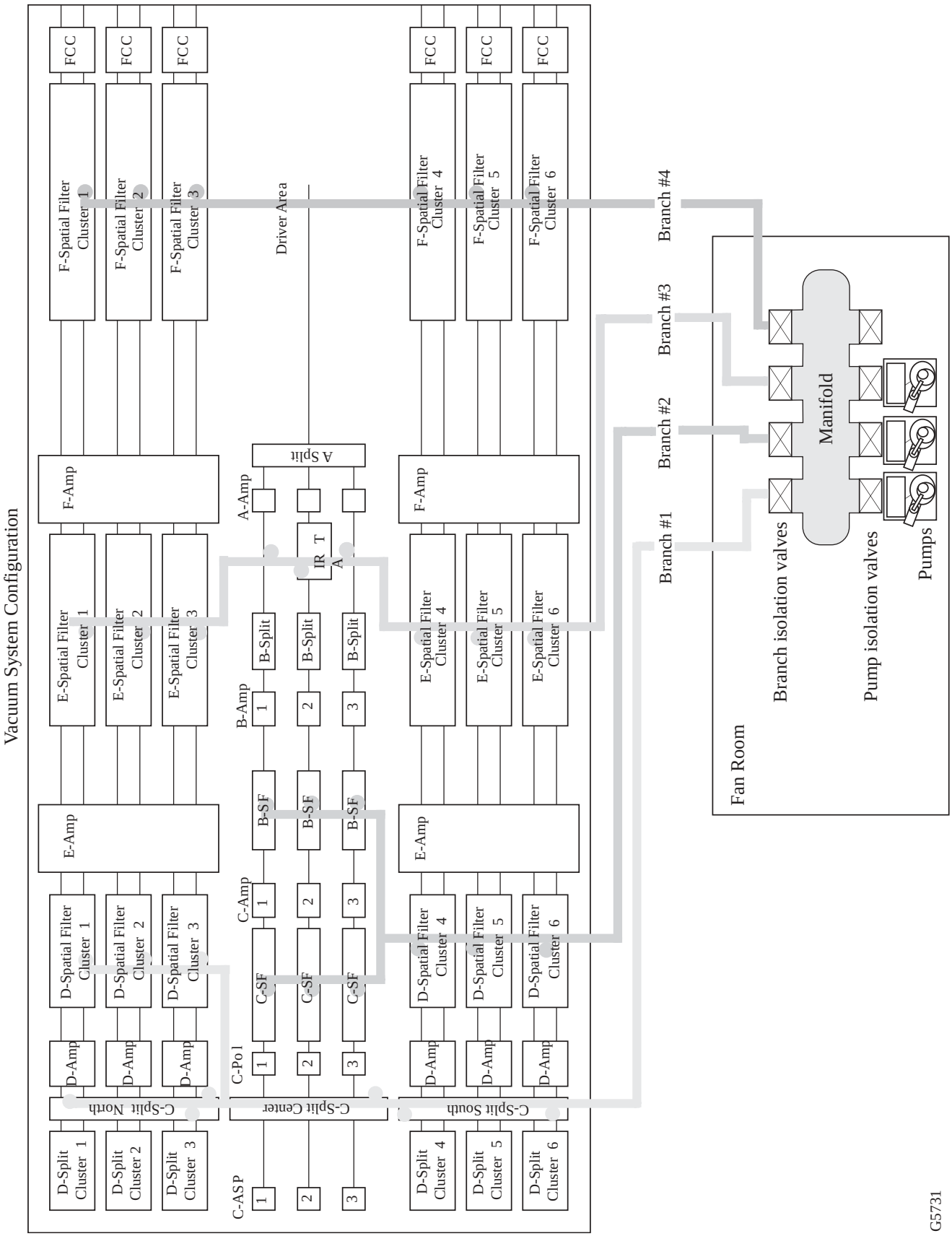

Figure 5.6-2
Layout of spatial-filter vacuum system in the LLE building.

interface directly to 10-ft.-long, 6-in.-diam "riser" manifolds that service each of the 33 spatial-filter and relay structures. Each structure manifold has a single valve for all of the filters in that structure (five or ten). The filters are connected to the manifolds by 1.5-in. vacuum flex lines. Figure 5.6-3 is a photograph of a typical spatial-filter structure, showing the vacuum manifold arrangement. The entire system with 243 filters can be pumped to base pressure in 90 to 120 min, and any single group of ten filters can be pumped in 3 to 20 min. Initial pumping of the entire system would normally be accomplished with two pumps operating; however, the system operating pressure of 2 mTorr can be maintained with a single pump. These capabilities ensure that a filter, or group of ten filters, could easily be serviced within a 1-h shot cycle, if necessary. Furthermore, with four pumps available, any one of the pumps can be maintained without interrupting system operation.

G5732

Figure 5.6-3
Spatial-filter structure with vacuum manifold riser.

5.7 FREQUENCY-CONVERSION CRYSTALS

The FCC's convert the fundamental wavelength of the OMEGA laser (1054 nm) to the second- (527-nm) and third- (351-nm) harmonic wavelengths. The FCC assemblies were designed and built to meet the requirements established in the OMEGA Upgrade Preliminary Design Document[1] and have subsequently been upgraded to incorporate a second tripler crystal and improved moisture protection. The FCC's are located in the beamlines in the Laser Bay, directly following the stage-F spatial filter near the final image plane of the system. The OMEGA system performance specifications call for routine energy-conversion efficiency to be ≥70% for 1-ns pulses (conversion efficiency is a function of intensity and, therefore, for longer pulse lengths the conversion efficiency decreases), with peak conversion about 80%. Though this is not difficult to attain with any single FCC unit, it is important that all 60 units perform similarly, to maintain beam-to-beam energy and power balance.

To keep losses below 0.5% of the conversion efficiency at the peak of the main pulse, where the crystals are the most sensitive to errors, the following tolerances (obtained from Table 7.4 of Ref. 1 with adjustment where appropriate by the crystal thickness ratio 12:7.6) must be achieved:

- Doubler misalignment 142 μrad
- Doubler wavelength shift 7 Å
- Doubler temperature 0.6°C
- Tripler misalignment 29 μrad
- Tripler wavelength shift 0.2 Å
- Tripler temperature 0.1°C
- Second-tripler misalignment 100 μrad
- Second-tripler wavelength shift 0.6 Å
- Second-tripler temperature 0.3°C
- Polarization angle ±0.3°
- Fraction in wrong polarization 3×10^{-5}

The desired 1%–2% rms level of irradiation uniformity on target imposes strict fabrication, assembly, and operating tolerances on the FCC's. The generation of 60 near-identical beams thus requires that each beam is frequency converted under near-optimum conditions.

The design approach is summarized below:

- Angular tuning: This is accomplished with a motorized gimbal mount that can be adjusted to achieve the precise tuning angle with respect to the incident IR beam and to compensate for required changes of tuning angle with respect to temperature.

- Wavelength: The tolerances for wavelength shifts in the driver oscillators were determined for optimal tuning. These tolerances are within the state of the art for oscillator control, and the OMEGA oscillators are diagnosed and controlled to this accuracy.

- Temperature: In order to establish and maintain correct tuning, the crystal temperatures must be maintained to a tolerance of 0.1°C. Having the FCC's mounted in a closed structure within the Laser Bay helps to minimize temperature changes. The mounts and their housings are designed with this requirement in mind, and temperature sensors are incorporated into the mounts. The FCC controls are designed to perform angular tuning of the crystal gimbals in proportion to temperature changes.

- Polarization: The incident polarization contrast is improved with a Brewster-plate linear polarizer just ahead of the FCC's. The *p*- to *s*-polarization contrast after the stage-F spatial filter is designed to be about 100:1, and the 500:1 plate polarizer improves this to the required level (i.e., $\leq 3 \times 10^{-5}$ of the energy in the undesired polarization). Adjustment of the incident polarization angle to the crystal axes is carried out by rotating the FCC gimbal rings with respect to the plate polarizer, as a one-time setup adjustment. A UV absorption window is mounted just ahead of the first conversion crystal to minimize the effect of reflected UV energy on the polarizer coating.

- Crystal thickness: The product $\Delta(KL)$, where K is the intrinsic nonlinear coefficient and L is the crystal thickness, represents the effective conversion "strength" of the crystal and should ideally be

the same for each crystal to within 0.5%. It is minimized by keeping the errors in the crystal thickness, and in the angle at which the crystal is cut, at or below 0.35% each. This represents a 2.4° tolerance in θ and a 50-μm thickness tolerance. During fabrication of the initial crystals, the thickness tolerance was loosened because calculations on beam balance indicated that this was sufficient if crystal pairs were matched to achieve an overall rms error of ≤200 μm.

Frequency-Conversion-Crystal Assembly

The FCC assembly, which includes the 28-cm-clear-aperture polarizer, the gimbal, and the IR absorption glass, is shown in Fig. 5.7-1. It is designed to fit into a space allocation comparable to that of an OMEGA rod amplifier, which is limited to a height of 60 cm. Each assembly is mounted in a five-level box structure, which is enclosed for thermal isolation. The FCC gimbal and polarizer are supported by a high-stiffness-steel rail, which includes adjustments for tilt and centering. The entire assembly is designed to allow the rail and polarizer to be installed and leveled in the structure and then aligned to the beam. The FCC gimbal, which holds three crystals and the UV absorption window, is assembled separately and the crystals are aligned to each other. The gimbal is then tuned for near-optimum UV conversion using 100-ps laser pulses. The unit is then installed on the rail in OMEGA and aligned.

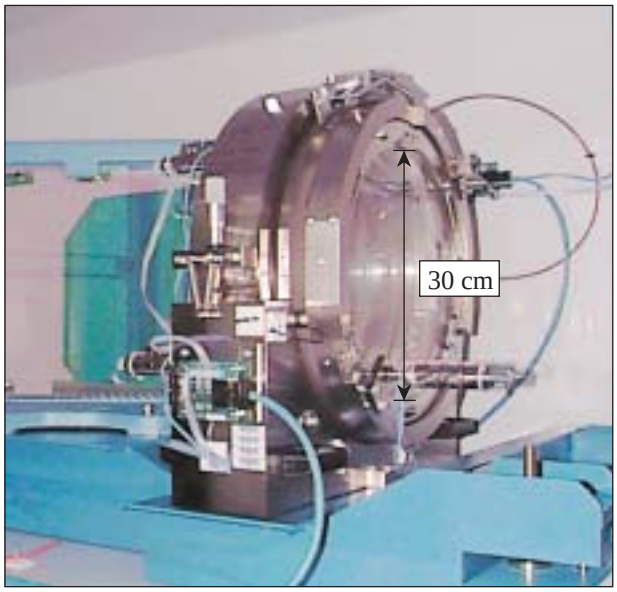

E10382a

Figure 5.7-1
FCC assembly.

The FCC's are made of potassium dihydrogen phosphate (KDP) and are 300 mm in diameter. The doubler and first tripler have an average thickness of 12.2 mm, and the second tripler has an average thickness of 10 mm. The crystals are grown in large boules, each yielding 10 to 12 blanks, which are cut and shaped. Their faces are then precision diamond machined or polished to within 0.1 mm of the specified thickness, with a surface roughness of about 50 Å (rms). A protective layer of GR650 or PMMA is applied, in addition to the sol-gel coating, to block moisture from reaching, and subsequently damaging, the KDP substrate. Due to the crystalline nature of the KDP and the difficulty of finishing it, the final transmitted wavefront error for most crystals is $\lambda/3$ @ 633 nm.

The KDP crystals are mounted in cells, which are then bolted together. The doubler is mounted such that it has a fixed wedge of 0.5° with respect to the first and second triplers. This setup along with the UV absorption window makes up an FCC. The crystal axes are oriented at 34.8°±0.1° with respect to the incoming *p*-polarized beam in the manner shown in Fig. 5.7-2, and the *e* and *o* axes are aligned to each other to within 0.1°. Provision is incorporated in the mount design for the crystal cells to be precisely adjusted with respect to each other using a micrometer during the tuning process. After the crystals are adjusted with respect to each other, they can be rotated in unison to achieve the 34.8° rotation angle to the polarization vector.

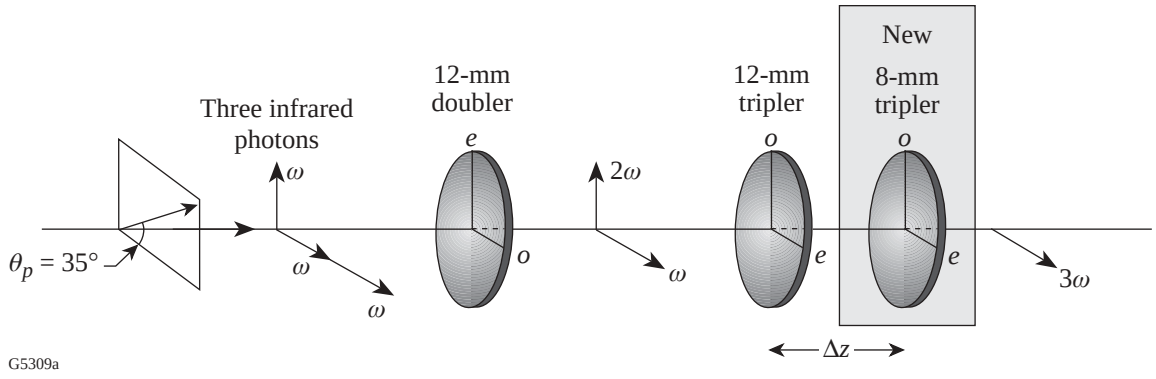

Figure 5.7-2
FCC crystal orientation.

The UV absorption window, made of type-F11 optical glass from Ohara, is designed to transmit the incident IR light from the laser, but to reflect and absorb any UV light reflected from the target or any optical surfaces. The window has a 50% reflective coating for 351 nm on the side facing the crystals, and it absorbs 99.9% of any UV entering the glass. In this manner it protects the dielectric thin-film polarizer coating from damage due to UV light, for which its threshold is ≤0.1 J/cm^2. It is also possible to use the window's UV reflective surface as an alignment reference if necessary. The reflection off of the surface of the window is aligned to that of the first and second triplers, thus making it possible to coarse align the crystals to their retro position using the UV alignment laser from the Target Bay if necessary.

The FCC assembly also includes an IR absorber. This 14-in. × 20-in. × 0.5-in. glass plate is mounted beside the polarizer and is designed to absorb IR reflections from the coated surface of the polarizer. The glass, called Azurelite™, is an architectural glass that has high absorption (OD ≥5) at 1054 nm and is AR coated for a 33° angle of incidence. This absorber serves to minimize the possibility that IR energy rejected from the polarizer (worst case: 40 J) could vaporize finished surfaces inside the enclosure and cause contamination of optical surfaces in the enclosure.

FCC Thermal Enclosure

The FCC assemblies must be operated in a thermally stable environment, and the KDP crystals should not be exposed for more than a few minutes to a relative humidity higher than 50%. To achieve this, ten assemblies are contained (five high × two wide) in each of six structures that are surrounded by

a thermal damping enclosure, as shown in Fig. 5.7-3. Fixed panels on the beam input and output ends have 14-in. apertures to allow the beams to pass. The sides of the structure have upper and lower pairs of hinged doors that allow the FCC assemblies to be serviced. The enclosure panels are made of 1-in.-thick, high-density styrofoam insulation, encased in painted sheet steel. Inside the structure, each of the ten FCC assemblies is isolated by 0.25-in. sheets of ABS plastic, and the top and bottom are closed off with insulated panels. Detailed thermal analysis has shown that the structure enclosure provides damping of the variations in the Laser Bay environment (70°±0.5°F) adequate to keep the crystal temperature stable even with the 14-in. input/output apertures. Beam tubes that extend from the stage-F spatial-filter output lenses to the FCC structure input have been added, however, both to minimize air currents and to protect the lenses. In addition, doors installed on the output end can be closed to minimize air flow into that end of the enclosure. These doors are pneumatically controlled and shut automatically in the event of a power failure to prevent any significant changes to the crystal environment. The doors can also be closed during maintenance shutdown periods to keep the crystals protected. The output doors have a Pyrex™ window for each beam to allow for visual inspection of the FCC optics (for gross damage or obstructions) with the doors closed. To prevent the system from being fired with the doors closed, a hard-wired relay in the door control electronics unit prevents the system from propagating a high-powered beam (but not from firing the amplifiers) with the doors closed.

G5733

Figure 5.7-3
FCC thermal enclosure.

FCC Tuning

To achieve high-efficiency frequency conversion, the KDP crystals must be correctly oriented with respect to the optical axis of the incident 1054-nm laser beam. To achieve this, the doubler/triplers *e* and *o* axes must be set at 34.8° with respect to the incident polarization vector, and the crystals must have their *e* and *o* axes exactly orthogonal (≤0.1°), as shown in Fig. 5.7-2. In addition, the tuning angle for the crystal pair varies with temperature, so the temperature must be closely monitored to keep them tuned to peak performance. The tuning process occurs in three steps: initial FCC tuning and alignment of the retroreflection of the UV window, transferring the gimbal to the structure and aligning the gimbal to the beam, and final high-power tuning. Once the best-tuned position is found for a particular temperature, angular tuning of the crystals as a function of the FCC gimbal temperature can be performed prior to a system shot.

The initial tuning process is done off-line. First the doubler and the triplers are mounted in their respective cells; the fiducial mark indicating the *e* axis on each crystal is aligned with a respective fiducial mark machined into the cells at the proper rotational angle. (The fiducial marks are accurate enough, but the cells can be fine adjusted to achieve orthogonality with a micrometer if necessary.) The UV absorption window is mounted in a fourth cell that contains its own angular adjustment screws. This cell is then attached to the three cells that contain the doubler and the two triplers. The crystals and window cells form the inner ring of a two-axis gimbal with actuators located in line with the *e* and *o* axes of the crystals. These actuators control the gimbal as a whole and will rotate all four cells in unison. A third actuator is installed on the output side of the gimbal. This allows the second tripler to move independently about its *e* axis. The gimbal rings also rotate about the optical axis to allow for fine tuning of the *e* and *o* axes with respect to the polarization vector. The assembled gimbal is placed on a pre-aligned FCC rail, with a polarizer, in a tuning setup that uses 5-hz-rep-rate pulses from a regen. The *o* axis of the doubler is aligned orthogonal to the *o* axis of the triplers using image analysis of nonlinear isogyre patterns obtained with an OMA camera. The *o* axis of the doubler is then aligned 34.8° (±0.1°) from horizontal (the direction of polarization) using the same technique. Scans are then performed to determine the peak-tuned positions of the doubler, first tripler, and second tripler. Once the correct angular positions (i.e., actuator settings) are determined, the retroreflection from the UV window is set parallel to that of the tripler, using an alignment telescope.

The second step is to install and align the gimbal in the FCC structure. This is a two-step alignment process that occurs once the pretuned gimbal is installed on the FCC rail. The gimbal and the polarizer are bolted to the rail and the polarizer is preset to its highest contrast angle. The assembly is then “IR aligned,” which refers to centering the gimbal to the input beam and pointing the rail. The rail is leveled to ≤0.1° and then pointed using cross hairs to within 0.5 mm. The gimbal is then “UV aligned” using a device called STAD (second tripler alignment diagnostic). STAD uses a 780-nm diode beam that is coaligned with OMEGA’s IR cw alignment beam to find the retro position of the doubler and the triplers. (A 780-nm beam is used due to the reflective properties of the coatings on the crystals.) Once the retro position of the crystals is accurately determined, the peak-tuned actuator setting is used to move the crystal to its nominal tuned position. All other crystal positions are calculated with respect to the peak-tuned position.

The final step in the integration process is to check the performance of the crystal at high power. The crystal is first ramped (i.e., shot at 1/4, 1/2, 3/4, and then full power, respectively), and performance of the crystal is monitored. During the ramping process, the axes of the FCC are adjusted, if necessary, to achieve higher frequency-conversion efficiency. If, after the ramping process, it is determined that

additional tuning is necessary, minor adjustments are made to the crystal axes (to avoid significant UV energy loss) until the maximum frequency-conversion efficiency as a function of FCC angle is established.

FCC Controls

The left-hand part of Fig.5.7-4 shows the two control interfaces to the FCC gimbals that provide for adjustment of the gimbal actuators and continuous temperature monitoring. The temperature of the crystal cell is monitored with a thermistor, which is connected to a remote sensing head (RSH), and interfaced to the executive control computer through a generic A/D module (GADM). Temperature is monitored and averaged continuously, and deviations from nominal (defined to be 70°F) are compensated for by adjusting the crystal tuning angles just prior to a shot. The dc motorized actuators are controlled through a standard dual-axis control module (DACM). Angular changes in the tuning are computed with respect to temperature change in the executive software; then the actuators are operated through the DACM.

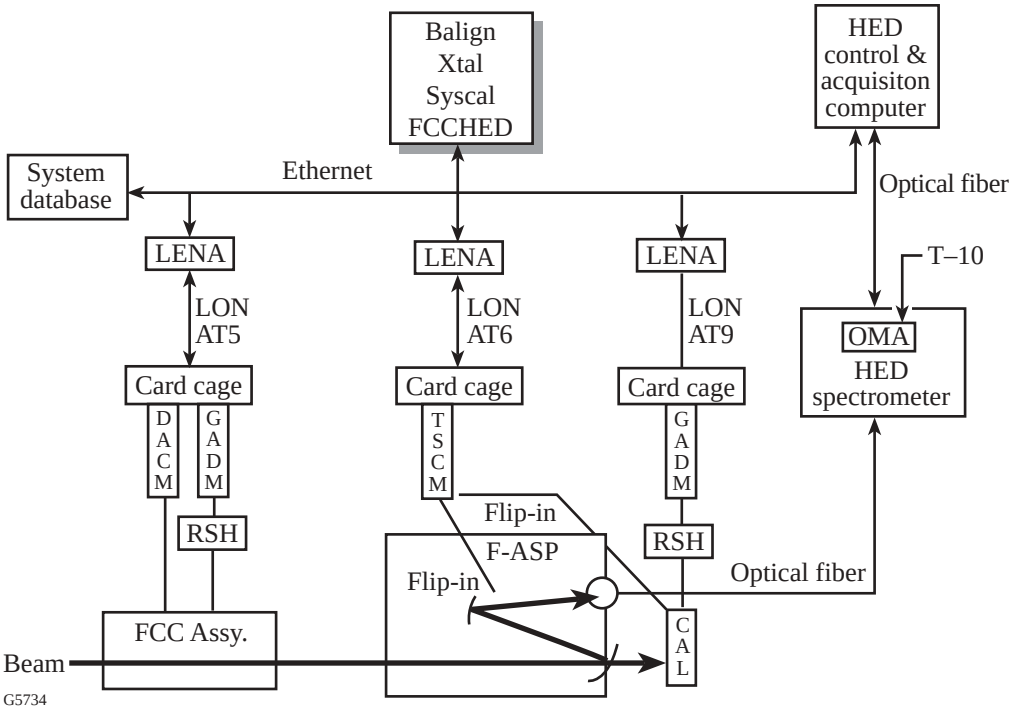

Figure 5.7-4
Control interface to FCC assemblies and the HED and system calorimeters.

5.8 SYSTEM ALIGNMENT

End-to-end alignment of a frequency-tripled, IR laser system such as OMEGA presents a difficult problem because the relatively low-power, cw IR alignment laser will not be converted to UV by the FCC's. This, along with the low IR reflectivity of the UV transport mirrors in the Target Bay, means that a single alignment beam cannot be used to align the system from source to target.

The OMEGA alignment system therefore uses separate IR and UV lasers to align the corresponding portions of the system. While this increases the system complexity, it eliminates the two disadvantages of single-wavelength alignment: the transport mirrors do not need dual-function (IR/UV) coatings (because UV light is used to align these optics), and the focus lenses need not be translated after IR alignment to compensate for chromatic shift. The former dramatically improves the damage threshold of the UV coatings, and the latter improves the operational accuracy of alignment. The IR alignment source is a mode-locked, cw, 1054-nm Nd:YLF laser. It is used with ASP's located at stages A, C, and F within each beamline. UV alignment utilizes a full-aperture, 351-nm cw laser that is injected into the beam after the FCC's and just before the achromatic F-ASP's. This is done with movable mirrors located in the Target Bay on the PMA. Co-alignment of this injected beam to the IR pulsed beam is performed using the F-ASP. An ASP located on the UVAT measures the alignment of the injected UV beams onto the target.

IR Alignment

The following basic processes are necessary to routinely align the IR beamlines:

1. Laser drivers and IR alignment laser injection (1 beam each)
2. Stage A–C pointing and centering (15 legs)
3. Stage C–F pointing and centering (60 beamlines).

Each process involves five steps: setup, image analysis, action determination, action implementation, and confirmation.

Process 1 requires the alignment laser and driver to be injected into the A-splitter, using the A-ASP. The ASP has pointing and centering references to ensure that the beam entering the stage-A splitter has the correct direction and position for propagation down the beamlines. The driver injection is done after the alignment of the laser driver (not part of this procedure) and is necessary to propagate a driver beam into the laser chain. The backlighter driver is injected into the middle A–C legs and is aligned by a stage-C ASP. This injection is largely a manual process.

Process 2, the alignment of the leg from the stage-A splitter to stage-C ASP, involves the alignment of the beams propagating from east to west in the Laser Bay and is performed using the alignment laser after it has been injected. For a given leg, this process involves the following hardware and is depicted in Fig. 5.8-1:

• A Splitter	• B Splitter	• C Amplifier
• A Amplifier	• B Amplifier	• C Spatial Filter
• A Spatial Filter	• B Spatial Filter	• C-ASP

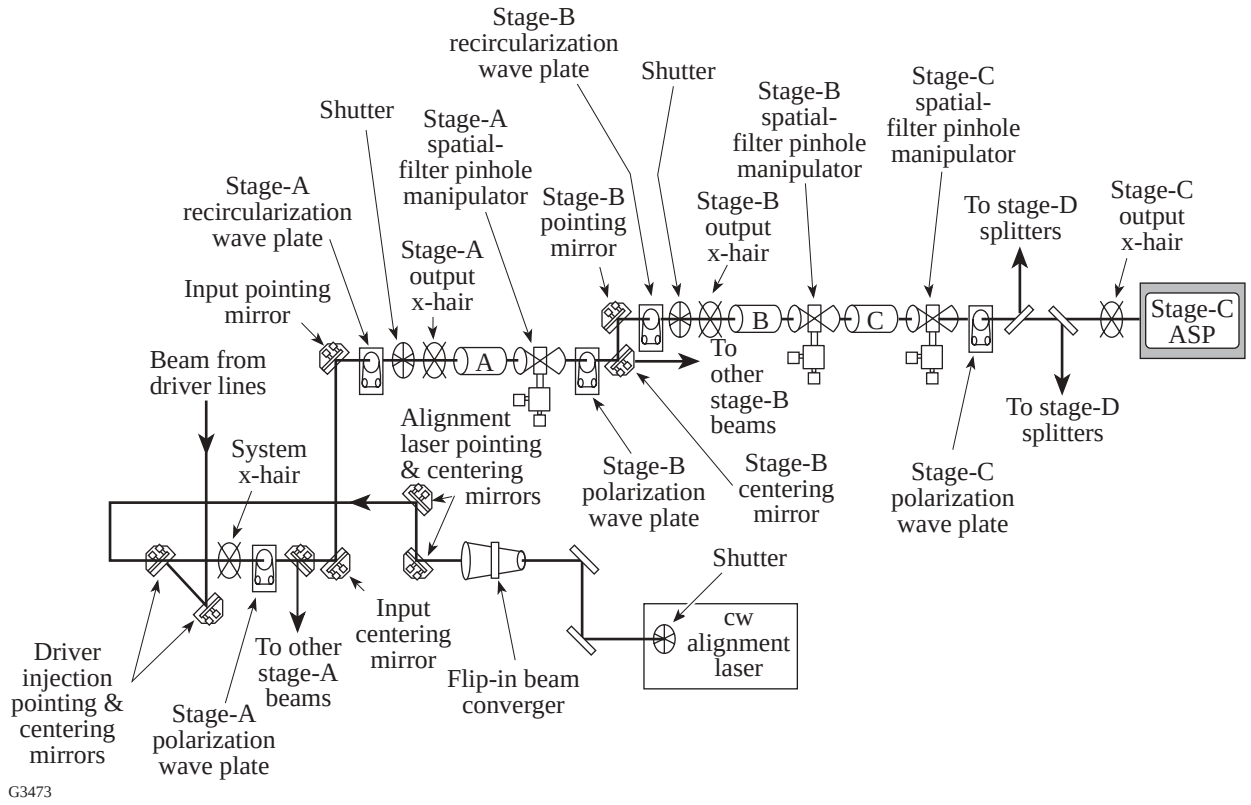

Figure 5.8-1
The optomechanical devices in an OMEGA beamline from the laser driver to stage C.

Process 3 aligns the last portion of the IR system, the stage-C splitter to F-ASP, and involves the following hardware as depicted in Fig. 5.8-2:

• C Splitter	• E Amplifier	• F Amplifier
• D Splitter	• E Spatial Filter	• F Spatial Filter
• D Amplifier		• F-ASP
• D Spatial Filter		
• FCC Structure		

When all three sections are aligned, the operator is assured that the centering reference at the end of the driver line has been transferred (within tolerances) to the centering fiducials at the F-ASP. This, coupled with the intermediate centering checks, ensures that the beam will not be vignetted on any optics in the laser chain. Similarly, the beam pointing in all stages is checked, corrected, and verified. The final IR pointing and centering positions at the F-ASP are recorded to be used as a reference for the UV alignment process.

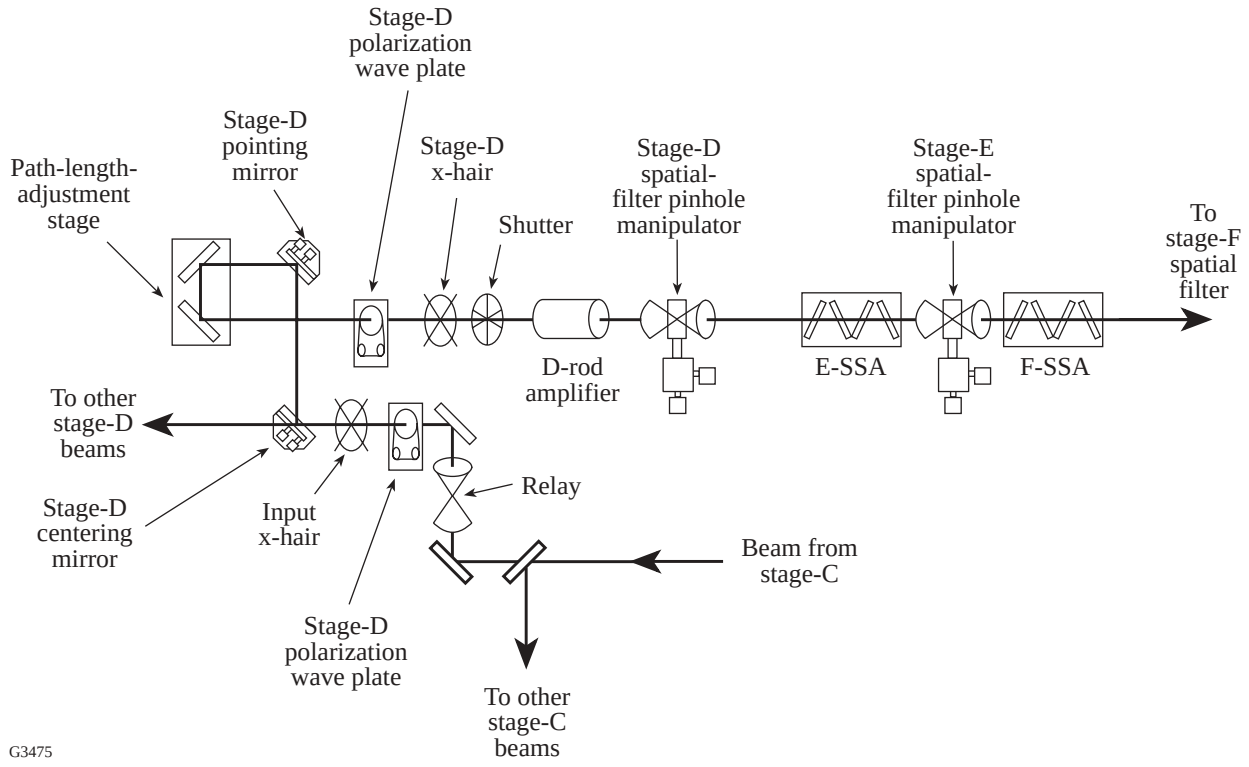

Figure 5.8-2
The optomechanical devices in an OMEGA beamline from stage C to stage F.

UV Alignment

Figure 5.8-3 depicts the optical configuration for alignment of the UV transport system. The periscope mirror assembly (PMA) and the F-ASP are major elements in the UV alignment scheme. The PMA is a system that positions a set of mirrors near the face of the shield wall in front of the F-ASP's. In each position, these mirrors form a periscope that injects a UV alignment beam, which originates on the UVAT, into one of the 60 beamlines at the input end of its F-ASP. After the UV beam is correctly aligned to the fiducial in the F-ASP, it is transmitted to the target chamber and retroreflected (from a surrogate target) to a video camera that is part of the UV-ASP on the UVAT. (The beam may also be transmitted to the UVAT via the opposing beamline that has also been accessed by the PMA.) The video signal is processed to provide position-error data that is used to drive the motorized end-mirror and target-mirror mounts to correct the pointing and centering of the beam or to adjust the focus lens in the FLAS. The PMA mirrors are then repositioned to inject the alignment beam into another beamline.

The following basic processes are necessary to routinely align the UV optical trains to correctly deliver the shot pulse to the target:

1. UVAT laser injection
2. UV transport system pointing and centering
3. Focusing

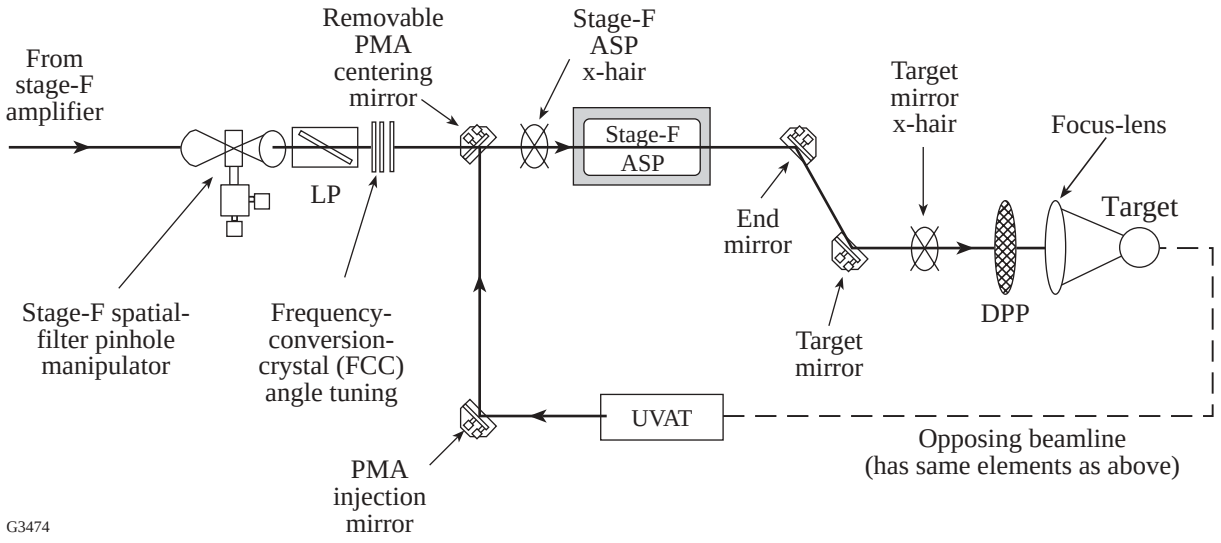

Figure 5.8-3
The optomechanical devices in an OMEGA beamline from stage F to the target.

As with IR alignment, each process involves these five steps: setup, image analysis, action determination, action implementation, and confirmation. Here each process is performed on the 60 separate beamlines, and the setup step includes positioning and adjusting the PMA mirrors.

Propagation of Centering Errors

During the injection alignment, the alignment table and driver fiducials are centered on the system fiducial (in the A splitter). In the A to C-split alignment, the system fiducial is centered to the A fiducial and the A to the B fiducial. The C-split to F-ASP alignment centers the B-splitter fiducial to the D-splitter fiducial and confirms the D-splitter fiducial to the F-ASP fiducial for final IR centering.

The UV targeting process centers the F-ASP fiducial to the target mirror fiducial resulting in four stages where centering errors can occur: (1) driver to system, (2) system to cluster, (3) cluster to PMA, and (4) PMA to target mirror. The first transfer is done to avoid using the driver line for beam alignment, and so that injection need not be done at the C-ASP's. The second is necessary because the system fiducial is not at an image plane and lacks sufficient image quality for alignment past the A-split. The third transfer is necessary because targeting must be done in the UV. The final transfer is used to center the target mirror and the FLAS.

Wherever possible, alignment is performed in parallel steps across the beamlines to minimize the time needed to align the entire system. It is intended to utilize the parallel structure of the control network and the image processing to minimize the time required for each alignment step. The capability to align individual or subgroups of the beamlines is still required, even though the alignment hardware is not used to its maximum efficiency.

Infrared Alignment Table (IRAT)

The IRAT is the source for IR alignment and measurement of system collimation and wavefront. It is an optical system on a stand-alone optical table located near the stage-A amplifiers. Redundant

laser sources called Photonics I and Photonics II are provided. Both are Photonics™ cw Nd:YLF lasers that deliver 15 W of cw average power. The second laser source enables daily operations to occur in the event of one source failing. The IRAT optical system, shown in Fig. 5.8-4, has an output arm and a beam-return arm. The output arm has two stages of beam expansion and produces a collimated 60-mm-

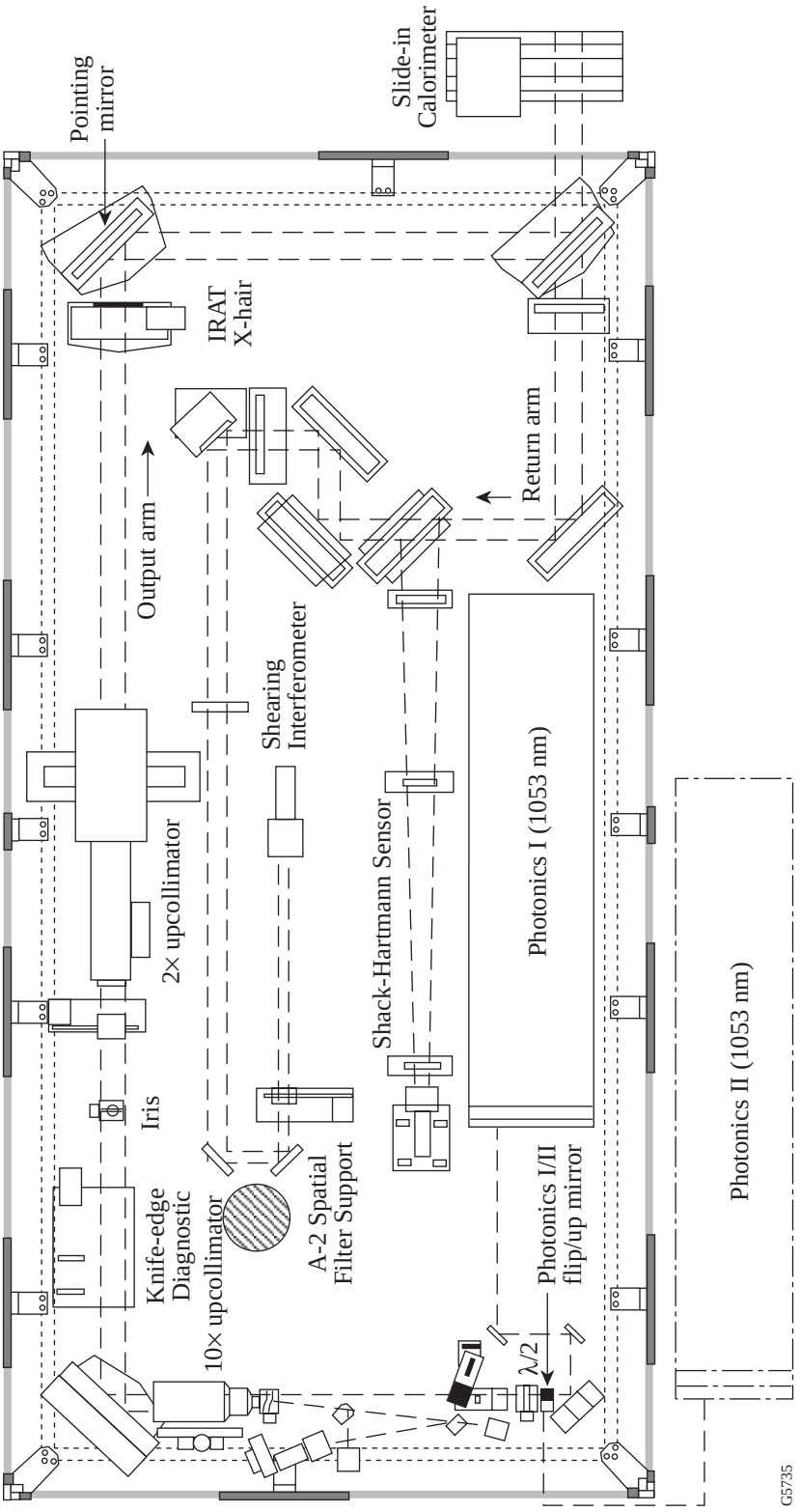

Figure 5.8-4
Optical layout of the infrared alignment table (IRAT). Both lasers have internal shutters that allow remote interlocking capabilities. (Note: Photonics II is shown on the south end of the IRAT for illustration purposes; it resides in fact on the west side of the IRAT)

diam output beam that is injected into the A-split structure. The output beam is aligned with the driver beam using the stage A-ASP. The alignment beam can be propagated through every beamline all the way to the F-ASP's. The return-beam arm is used to set the collimation of the system spatial filters using shearing interferometry. Shearing is accomplished by retroreflecting the alignment beam passing through any beamline filter(s) so that the near-collimated beam returns to the IRAT. The shear plate produces a shearing fringe pattern that is imaged on the CCD camera. Image analysis of the fringe pattern determines if the return beam is sufficiently collimated. The lens spacing on the spatial filter being tested is adjusted until 1/10 wave collimation is achieved. The interferometry subsystem was heavily used during system activation and remains in place for as-needed collimation checking of any beamline.

The system configuration is checked using the IRAT beam and associated diagnostics. The alignment of the system pinholes is checked with the use of the pinhole illuminator flip-in lens. The pinhole illuminator flip-in lens back-illuminates the system pinholes so that misaligned pinholes are visible when viewing the beam's image on the F-ASP camera. The knife-edge positions of the system pinholes are checked with a two-lens zoom setup called the Knife Edge Diagnostic (KED). The KED moves the focus inside each spatial-filter tube to the prescribed shot position. By scanning the pinholes across focus and examining the shadow created, the knife-edge positions of the system pinholes are verified.

The IRAT is also used as a reference for various diagnostics and systems. Integrating spheres used in the autobalance and beam balance functions utilize the IRAT as a reference signal for analyzing energy balance throughout the beamlines. The IRAT can also be coupled into a fiber launcher for use as an alignment source for remote alignment needs.

Alignment Sensor Packages

The term "Alignment Sensor Package" (ASP) is used to refer to the 79 functionally similar instruments within the OMEGA system. Seventeen of these are derived from the beam diagnostic packages used in the 24-beam system and are used in the driver line, stage A, and stage C. Sixty are integrated into the stage-F ASP structures, and two are included in the UVAT.

The ASP's are stable optical telescopes used to view an alignment beam propagating in a beamline. They diagnose the alignment of the system by sensing the pointing of the alignment lasers, and the position of the laser beam on optical components by sensing the position of alignment fiducials (e.g., cross hairs). These fiducials can be remotely inserted into the beamline or manually attached to optomechanical assemblies such as amplifiers and spatial filters. The ASP's are also used to view the position of the spatial-filter (SF) pinholes.

The ASP's are the primary sensors for the beamline alignment system and typically reside at the ends of the beamline segments. Each ASP contains a charge-coupled-device (CCD) television camera to view either the focus of the telescope objective (beam pointing) or the output image of the telescope to view the position of alignment fiducials (beam centering). Two-state devices move components within the ASP's to allow either of these functions to be performed by a single image sensor. The ASP's contain no moving or adjustable components between the entrance pupil and point where the beam focuses on an alignment reticle. This feature provides long-term stability of the pointing reference for the beam.

To establish and maintain the beam path, the ASP's are used to view flip-in fiducials (FIF's) at the start and end of each beamline. These FIF's were surveyed into place during laser system construction and then became the reference for subsequent alignments. To monitor beamline-centering stability and maintain the beamline geometry of the laser system, the ASP's locate the end fiducial relative to the image of the start fiducial.

Driver, Stage-A, and Stage-C ASP's

The driver, stage-A, and stage-C ASP's are highly stable optical packages that use a folded multi-element lens system, coupled with a solid-state detector, to sense pointing and centering. The top-level performance requirements for the driver, A, and C alignment sensor packages were derived from the pointing error budget that dictated the pointing sensitivity, short-term stability, and long-term stability (drift) for these instruments.

The design of the stage-C ASP is shown in Fig. 5.8-5 (the A-ASP and driver-ASP are nearly identical). The C-ASP components are built on a baseplate that provides a stiff mounting platform for the folded optical system. It is built and precisely aligned off-line, then installed as a unit and aligned to beamline fiducials. All components that could affect internal pointing are mechanically locked in place after bench alignment. The ASP has a flip-in centering cross hair and a shutter located immediately in front of the entrance lens. A 90-mm-diam collimated beam is centered at the entrance lens and begins to focus into the system. The converging beam is folded into the secondary and directed toward the beam splitter. The beam splitter reflects part of the light for the pointing arm and transmits the rest for the centering arm. The pointing beam focuses onto a fixed reticle, which is then imaged to the CCD camera. For centering, a moveable stage inserts a mirror pair in front of the CCD camera, blocking the pointing beam and folding the centering beam into the path. The centering arm images the entrance lens' cross hair onto the CCD camera. Since this sensor is used only for alignment, it is shuttered during a system shot to prevent laser light from entering the optical system and damaging the components or the CCD camera.

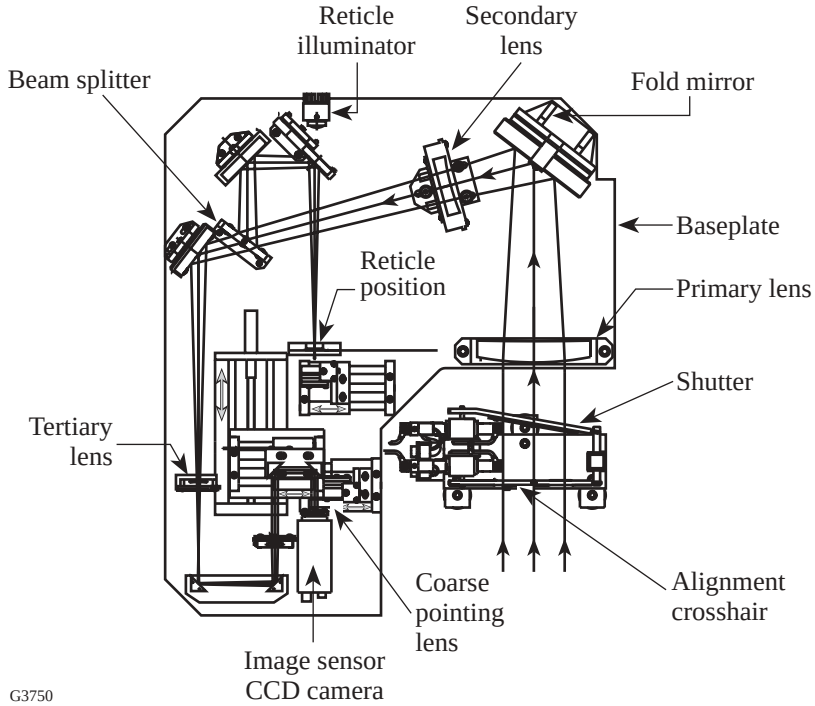

Figure 5.8-5
Stage-C ASP optical design.

The primary function of the driver ASP is to diagnose the alignment of the driver pulse. The driver ASP must sense pointing to 1.3-μrad accuracy over a 10-mrad field of view.

The stage-A ASP diagnoses the injection of the driver line and IRAT beams into the laser system. It is mounted in the stage-A splitter structure; it also is designed to sense pointing to 1.3 μrad over a 10-mrad field of view. This sensor must be able to diagnose beam centering (FIF position) to 0.13-mm accuracy and includes a collimation sensor to allow the collimation of the IRAT and the driver beams to be matched.

The stage-C ASP's diagnose the alignment of the beam legs from the B splitter to the C splitter. The stage-C ASP also must sense pointing to 1.3 μrad over a 10-mrad field of view and must diagnose beam centering (FIF position) and drift to 0.19-mm accuracy.

Stage-F Alignment Sensor Package

The F-ASP provides for pointing/centering alignment of the IR beamlines and co-alignment of the UV alignment laser beam to the IR beam train. The beam sampling pickoffs for each beam in the F-ASP structure provide inputs for the HED and other beamline diagnostics in addition to the ASP's.

The requirements for the stage-F alignment sensor package (F-ASP) were derived from the pointing error budget—a systematic top-down allocation of the top-level, 8.33-μrad pointing error to the various components of the laser system. The driving considerations were alignment precision (<0.3 μrad) and pointing stability (<2.7 μrad/h). The instrument is required to meet all three of these specifications. It was also required that the F-ASP use a bare glass reflection rather than transmission through a "leaky mirror" to provide insensitivity to wavelength, minimize polarization effects, and maximize radiometric stability. Therefore, the primary element (called the "primary pickoff") of the objective is a fused-silica off-axis paraboloid, with its uncoated concave surface facing the incoming beam. It reflects 4% (at all three wavelengths) into the F-ASP and is not polarization sensitive. The second surface is sol-gel AR coated (for 3ω only, SG3ωAR design) and is concentric with the first surface, forming an effective parallel plate that does not affect the collimation of the transmitted beam.

To maximize precision, the effective focal length of the F-ASP objective is matched to the pixel size of the detector. This, in combination with the requirement for complete absence of chromatic aberration, led to the selection of a three-mirror, off-axis, all-reflective telescope, with an effective focal length of 3.3 m, for the *f*/10 F-ASP objective [see Fig. 5.8-6 (a)]. The primary pickoff is concave, the secondary is a convex sphere, and the tertiary is a concave sphere. The system off-axis aberrations are balanced through the combination of curvatures and tilt angles, yielding a diffraction-limited focal spot. The final mirror is a flat surface that is used to point the focal spot onto the reticle. The use of a reflective telescope puts more-stringent requirements on the angular stability of the Optomechanical System than a refractive system would; this is compensated by the complete lack of chromatic variation of optical performance provided by an all-reflective system.

Located just ahead of the secondary mirror is a flip-in, flat pickoff that is placed in the beam during a system shot. This optic reflects 4% of the light from the primary pickoff into the HED arm of the F-ASP. The transmitted light is delivered to a streak camera port on the west face of the F-ASP structure. On the HED path, the reflected light, representing 0.16% of the total beam energy, passes through a focus inside a sealed vacuum tube, then forms an image of the system aperture at the rear surface of the HED integrating sphere. The light is then transmitted along a fiber to the HED spectrometer.

During a system shot, the energy in each of the three wavelengths is measured by the HED spectrometer, which is calibrated for absolute energy by the full-aperture calorimeters mounted on the F-ASP just behind the primary pickoff.

The F-ASP relay is shown in Fig. 5.8-6 (b). In the ASP path, the three-element objective focuses the alignment beam onto the fixed reticle. From that point, a relay subsystem is used to image the reticle (and focal spot) onto a CCD camera for coarse, medium, and fine pointing. The relay subsystem can also be configured to produce a centering image at the camera. In the coarse-pointing mode the subsystem provides pointing resolution of ±2 mrad with ±10-μrad precision. In the fine-pointing mode it has ±50-μrad range and ±0.3-μrad precision. The fine-pointing accuracy is required for both beamline pointing in the IR and precise co-alignment of the UV alignment beam to the IR for target alignment. Medium pointing is approximately 2× the field of view of fine pointing (1/2 the precision). When SSD modulation is used, system alignment is monitored with the F-ASP's in the medium-pointing mode. The wider field of view is necessary for viewing the larger system pinholes that are required when the SSD effect is present. All other driver configurations require the F-ASP's in fine-pointing mode.

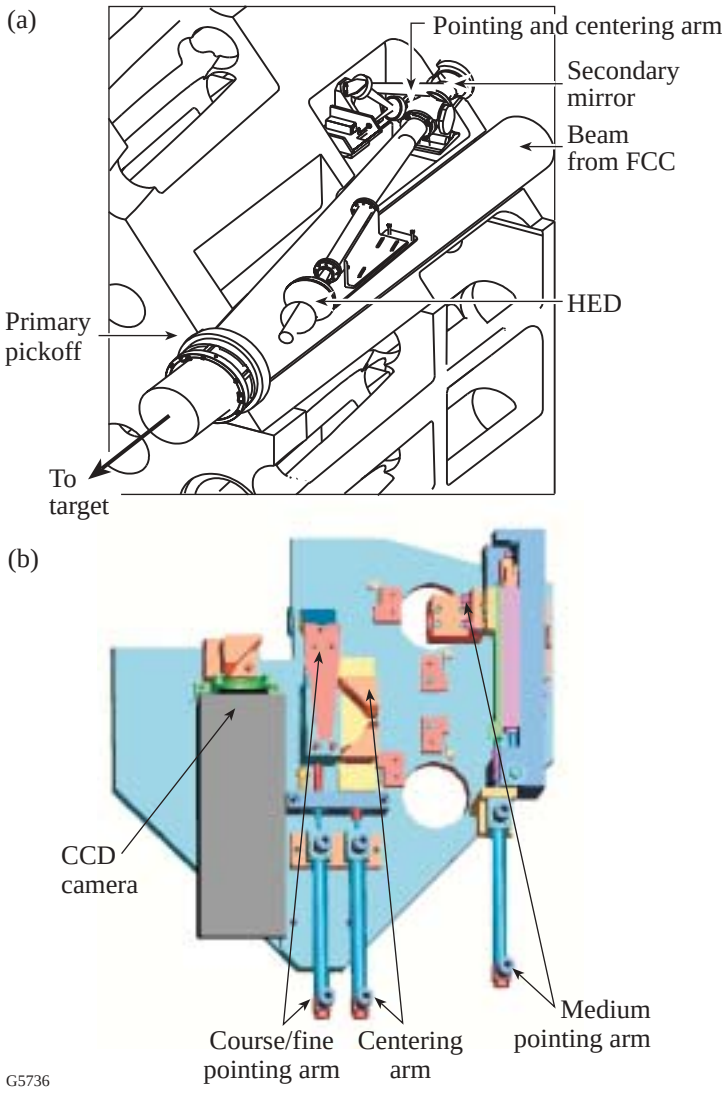

Figure 5.8-6
(a) Major optical components in a stage-F alignment sensor package (F-ASP) for a single beamline. (b) Components of an F-ASP relay system. Pneumatically driven optics allow the system to be configured in centering, coarse-pointing, medium-pointing, or fine-pointing mode.

The requirement for long-term pointing stability drove the mechanical design. In general, the need for extreme angular stability leads the mechanical designer to strive for symmetry in all possible aspects of a mechanical structure. The beam-to-beam spacing within a cluster caused adjacent F-ASP's to nest together in such a fashion that individual one-beam instruments would, necessarily, have been highly asymmetrical. To avoid this, ten-beam F-ASP units were designed with modular subassemblies that can be removed for off-line service as required. To further improve the stability of these instruments, the main structure is made of Harcrete™, a cast epoxy/granite composite. This material has the properties of high stiffness, low thermal conductivity, excellent vibration damping, excellent dimensional stability, and the ability to be cast into complex shapes. Figure 5.8-7 depicts two of the cast monoliths; the one on the right is sectioned to show the optics in a single F-ASP unit.

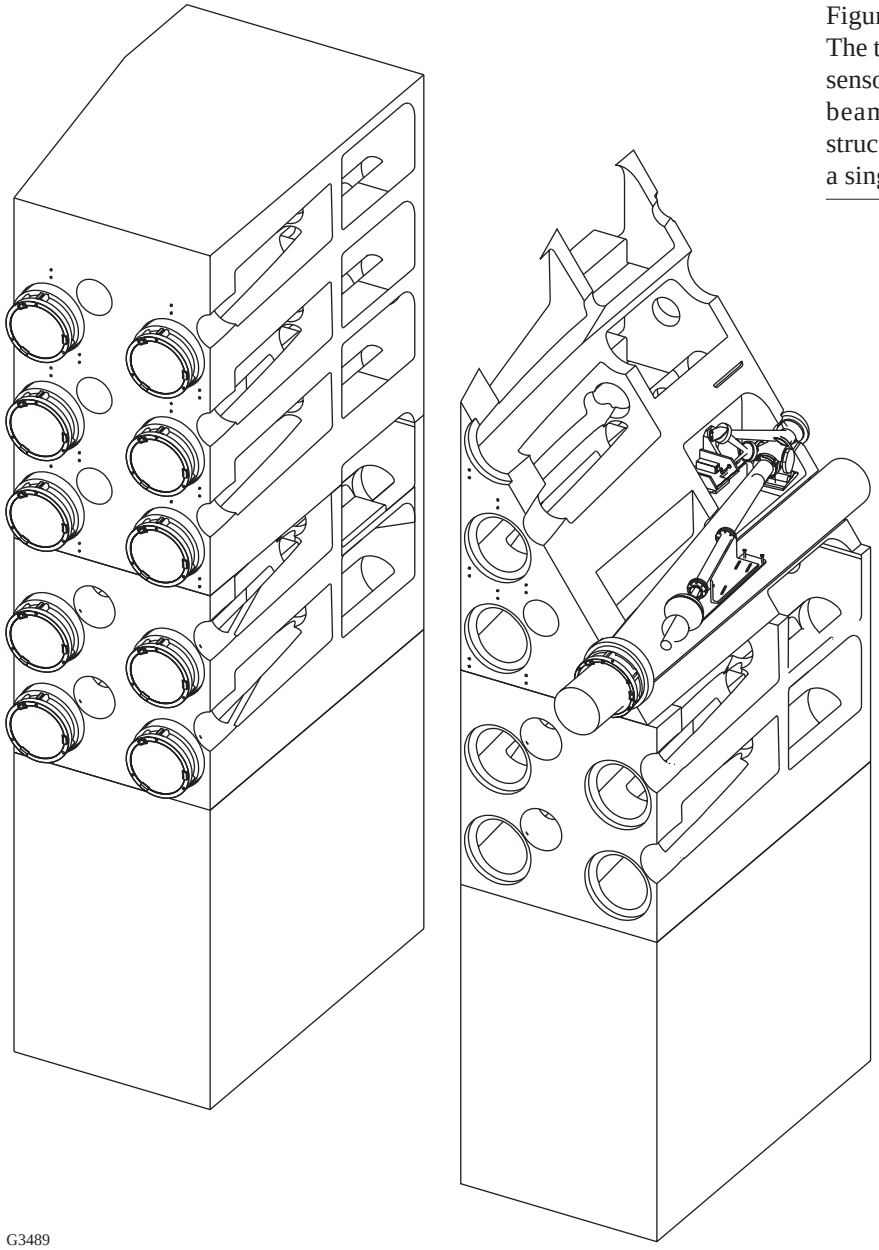

Figure 5.8-7
The two monoliths for the stage-F alignment sensor package (F-ASP), each containing ten beamlines. A section through the right structure depicts the layout of the optics for a single beamline.

To avoid the problem of post-adjustment drift, the critical optical mounts were designed to be nonadjustable. Adjustable installation fixtures used during installation permitted the optics to be positioned correctly and then epoxied into place, using special low-shrinkage, high-stability epoxy. The installation fixtures were then removed from the F-ASP. This method allowed the use of reasonable tolerances during manufacturing, while precluding drift during operation.

The moving parts of the F-ASP are components of modular subassemblies that can be removed for off-line service. The video camera, which may be the least reliable component of the instrument, is contained in the relay subassembly that mounts kinematically to the F-ASP. The reticle is the system reference and is fixed to the structure rather than to the relay subassembly. As a result, the camera can be changed without affecting the pointing reference. An off-line alignment fixture is used to adjust and test the relay so that it is correctly focused and aligned when inserted into the F-ASP structure.

Periscope Mirror Assembly (PMA)

The primary function of the PMA is to inject a full-aperture UV laser beam into the UV portion of the beamlines to facilitate alignment of these beams onto the target. This is necessary because the fundamental laser wavelength (1054 nm), which is used to align the IR beamlines, is not efficiently transmitted by the UV transport optics, and the focusing lenses are designed for the UV.

The 270-mm UV alignment beam originates on the UVAT and may be injected into any of the 60 OMEGA beamlines using two sets of mobile mirrors. Identical systems for the north and south halves of the Target Bay are used to reduce alignment time and, more importantly, to create a continuous optical path through opposing beams. The latter facilitates performing a multitude of alignment and calibration procedures that require reflected and transmitted UV beams. Each gantry has two mirrors that move independently to inject the UVAT beam into any of the 30 beamlines located on the north or south side of the Target Bay. Figure 5.8-8 illustrates the principal features of the PMA that services the north segment of beamlines (the south assembly is identical).

Requirements for the PMA were derived from the system-level, shot-cycle time and the pointing error budget. The following key requirements were the main drivers in the PMA design:

1. Average time to position the periscope mirrors and settle transients: ≤15 s

2. Alignment beam coarse-positioning tolerance (3 σ):
   - pointing ≤ ±1.8 mrad
   - centering ≤ ±1.0 mm

3. Alignment beam fine pointing (1 σ): ≤ ±3 μrad

4. Alignment beam pointing stability: Angular drift due to PMA effects must limit total excursion to within ±3.0 μrad (1 σ) for a period of at least 40 s after acquiring the desired beam axis. Here, drift applies to beam displacements having frequency components less than 60 Hz.

Personnel safety was given highest priority followed by schedule, cost, and reliability. Also, Target Bay space considerations mandated that the PMA be housed within a 1.2-m-wide corridor running along the west shield wall.

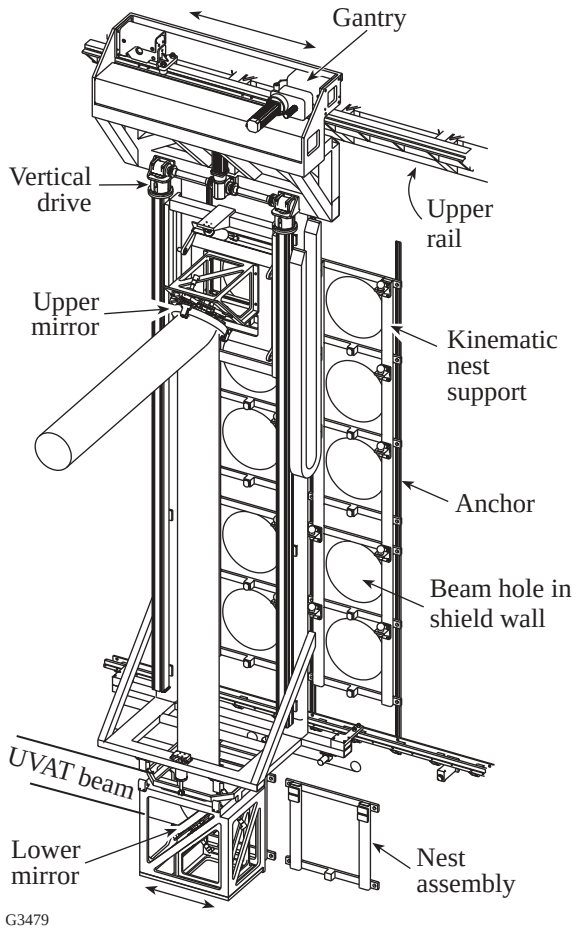

Figure 5.8-8
The major components for the north PMA. The entire gantry (with the lower mirror attached) moves to each of the six columns of five beams. The upper mirror moves vertically to select a particular beamline.

The pointing-stability requirement dictated most of this design. Based on a careful assessment of the expected shield-wall stability, kinematically ideal mounts were selected to support the periscope mirrors (5 cm $\times$ 35.5 cm $\times$ 51 cm) on the wall during alignment operations. Upper and lower periscope mirror modules (PMM's) are carried by a gantry that is a major feature of each PMA system. The lower mirror directs the alignment beam vertically upward to the upper mirror, which, in turn, reflects the alignment beam horizontally into the capture range of the F-ASP, i.e., into near coincidence with the desired beamline. Precision alignment with respect to the F-ASP is then accomplished by coordinated tip and tilt adjustments of both periscope mirrors using the F-ASP pointing and centering arms as references. The PMM's have built-in, two-axis micropositioners that operate under closed-loop servo control identical to those of the end and target mirrors.

A typical operation sequence for one of the gantries is as follows: Given a command from the host computer or a manual panel, the PMA local controller [a programmable logic controller (PLC)] activates the horizontal drive and moves the gantry along the wall, stopping at the desired column of five beamlines. While the gantry is traveling, the controller also activates a precision ball screw drive that moves the upper mirror vertically to the desired beamline. Both mirrors are then transferred to their respective kinematic nests on the shield wall and are released from mechanical contact with the gantry. This isolates the mirrors from disturbances that may otherwise be transmitted through the gantry structures. Using the F-ASP as a reference, the UV alignment beam is accurately coaligned with the primary beamline. Various alignment functions can then be performed on the UV transport system, many of which involve an ASP on the UVAT. When alignment operations at a particular beamline are complete, the mirrors are transferred back to their stowed positions aboard the gantry. The above sequence is repeated as needed for each of that gantry's 30 beamlines.

The time for repositioning at the next beamline is minimized (≤8 s) by using an efficient path through each 30-beam array. Although the array measures about 3 m × 6.7 m, maximum transport velocity and acceleration are only 23 cm/s and 15 cm/s^2, respectively. As a result, driving forces and transient disturbances are low despite the mass of the gantries (>900 kg each).

Coarse-positioning requirements were met by surveying each kinematic nest into position using a surrogate mirror at each position in turn. The positional requirements in this case were well within the capabilities of current surveying practice. For fine pointing, the PMM's incorporate the same design as the transport mirror mounts (TMM's) and TMM micro-positioners.

Many safety provisions have been factored into the PMA design: the PMA corridors are fenced off with safety chains; emergency stop buttons are located on the PMA controls; warning beacons and an audio alert are activated during PMA transit; mechanical sensors are fitted on both sides of the gantries to provide emergency stops; and video cameras view both corridors.

Ultraviolet Alignment Table (UVAT)

The UVAT is the ultraviolet alignment source for the Target Bay optical system. The system can be configured to use either a 7-W *Q*-switched diode-pumped laser or a 7-W flash- pumped laser to produce two full-aperture (280-mm), collimated, 351-nm beams for injection by the PMA into the beam paths. The primary functions of the UVAT are to sense centering on the target mirrors and focus lenses and to detect pointing and focusing on target. In addition, a reference integrating sphere is provided in each arm of the UVAT for use in conjunction with the OMEGA transport imaging system (OTIS) to measure the transmission of each beamline in the UV. Figure 5.8-9 shows the location of the UVAT in the Target Bay between the two PMA gantries. The sensors on the UVAT can be used to sense light going through the target chamber (i.e., transmission) or to look at light reflected back from a target.

Figure 5.8-10 is the optical layout for the UVAT, which is built on a 4-ft. × 17-ft. optical table. The nominal UV alignment laser is a *Q*-switched, diode-pumped, frequency-tripled source that exactly matches OMEGA's wavelength. An alternate flash-pumped, frequency-tripled laser can also be used for UV alignment purposes. Either source can be used for alignment via a flip-in mirror. Most alignment activities require only a fraction of the power generated by either source, so a half-wave plate in combination with a polarizer can be used to attenuate the beam. The beam from each source is expanded and apertured and the image of each aperture is relayed through the system. The 6-mm-diam beam is

split with a polarizer; the split ratio can be controlled with a half-wave plate. Each arm then uses a custom-designed lens and a 1.8-m-focal-length, *f*/6 aspheric focus lens (an OMEGA target lens) to create the 280-mm-diam collimated output beam. The return beam in each arm is sensed for pointing and centering by the ASP's. When DPP's are installed on the system, the larger-field-of-view DPP ASP is used only to detect pointing.

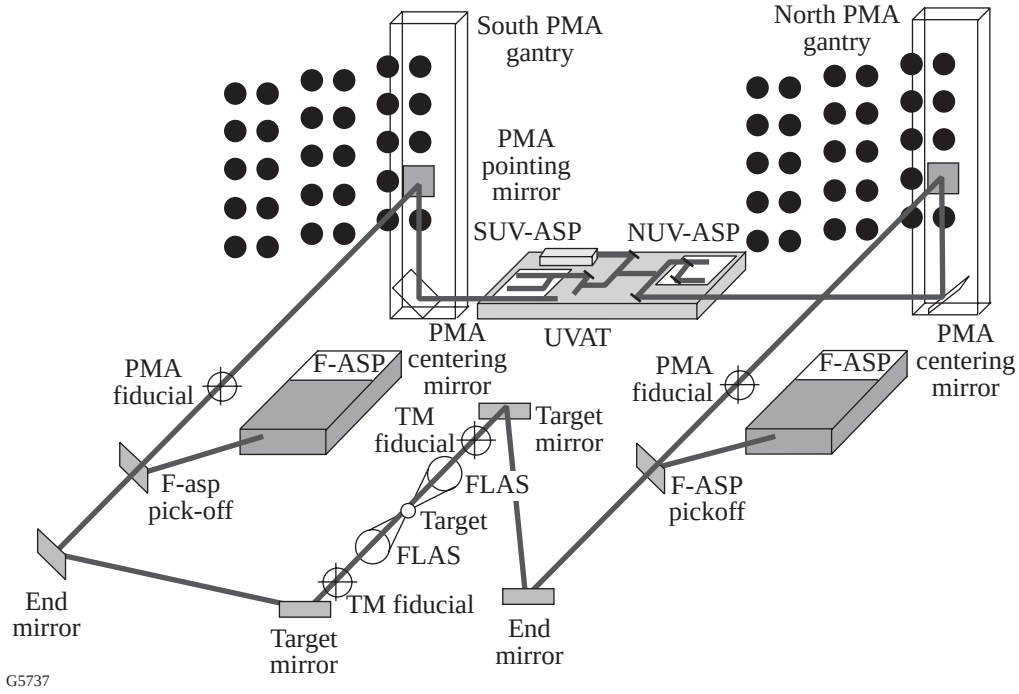

Figure 5.8-9
The UVAT resides on the west wall of the Target Bay, directly beneath the viewing gallery.

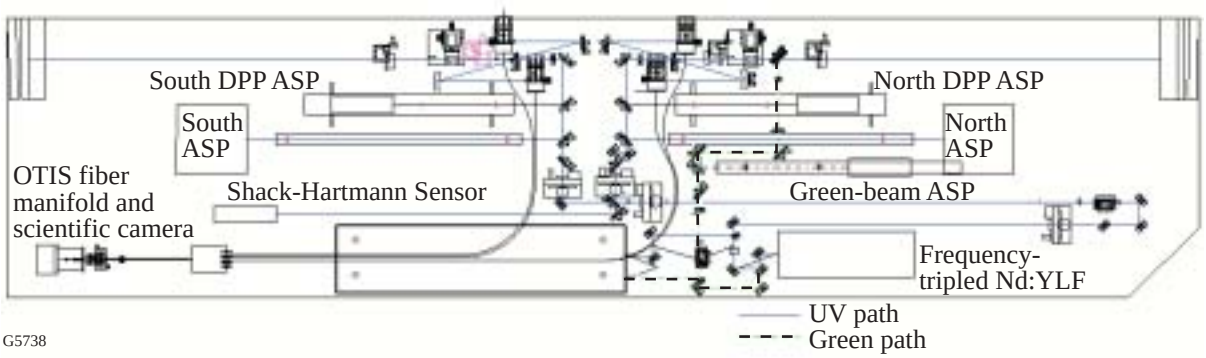

Figure 5.8-10
The UVAT provides two full-aperture UV alignment beams and has alignment sensors in both arms. The north arm can also produce a full-aperture green alignment beam.

5.9 TARGET BAY TRANSPORT OPTICS

The UV transport system utilizes two mirrors per beam to direct the 60 beams to the target. The two-mirror configuration was chosen for economy and to reduce the in-air path length of the UV beam. The latter was needed to ensure that the intensity–length product for the beam was below the threshold for stimulated rotational Raman scattering (SRRS).[7] Since UV light is used to align the UV transport system, the optical coatings for the transport mirrors were optimized for UV radiation only.

The task of mapping the 60 nearly parallel beamlines to the spherical target geometry had two fundamental constraints: all 60 beams had to have nearly equal path lengths and the incident angle on mirror could not be greater than 60°. Given these constraints it was a straightforward process to map a beam to a target port and then locate the end mirror along the beamline to obtain the proper path length.

For the sake of irradiation uniformity, an additional optimization was imposed upon the mapping. This entailed reducing the proximity of beams that share the same stage-A amplifiers. This reduces the effect that any variation in the performance of a single stage-A amplifier (distributed into 20 beams) has on target irradiation uniformity. A mapping that grouped many such beams in one area of the target would accentuate the effect that a stage-A amplifier has on target performance. To mitigate this effect, the beam mapping was arranged such that, for a given hexagon on the TMS, no more than three beams share the same stage-A amplifier. For the pentagons, only two such beams are allowed. Figure 5.9-1 is a sinusoidal projection of the beam locations indicating which beams share each of the three stage-A amplifiers.

The beam paths, as mapped by the above constraints, are shown in Fig. 5.1-3. Figure 5.9-2 shows the relative locations of all of the ports on the target chamber. The convergence of 60 beams in the existing Target Bay leads to a high density of beams. The need to place structures and mirror mounts in that volume without obstructing any beam placed significant constraints on the configuration of structures in this area.

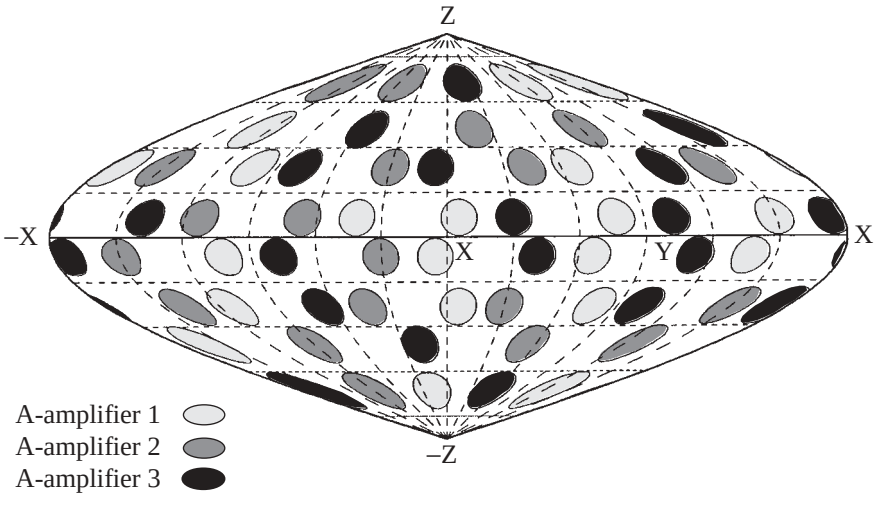

Figure 5.9-1
A sinusoidal projection of the beam locations on the OMEGA target sphere. Each beam is identified by the stage-A amplifier (three in total) from which it originates. The beam mapping was arranged so that any given TMS hexagon has, at most, three beams originating from the same stage-A amplifier; the pentagons have, at most, two beams.

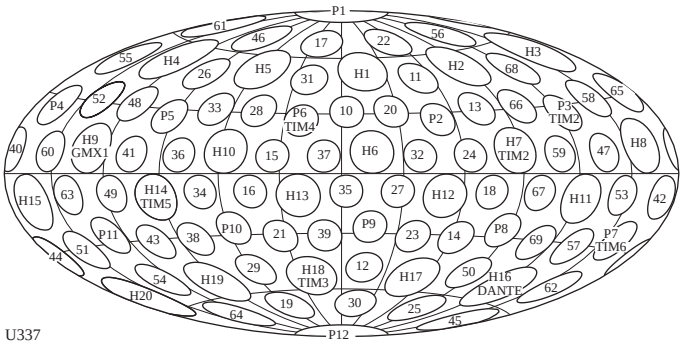

Figure 5.9-2
Relative locations of the ports on the target chamber. The beam ports are labeled with the "cluster, beam" beam designations defined in Fig. 1.3-3. The diagnostic ports are designated by the arrangement of beam ports that circumscribes them: H for hexagon, P for pentagon. These ports are numbered from the top of the chamber and CCW as viewed from the poles.

One effect of the mapping is that there is no systematic relationship between any given beam and the beam that enters the opposite port on the target chamber. Since this is important for a number of applications, the pairings are listed in Table 5.9-1.

Distributed Polarization Rotators

The function of a DPR is to aid in beam smoothing. It does this in combination with a DPP to achieve an even distribution of intensity values across the beam profile. The optic itself is a wedged birefringent crystal constructed out of potassium dihydrogen phosphate (KDP). The KDP wedge is 1 cm thick, 12 in. in diameter, sol-gel coated (with a GR650 or PMMA moisture barrier), and has a wedge of 4.5 arc min (1.3 mrad). It is mounted into an aluminum ring in a pneumatically driven slide that allows it to be inserted into the beam or removed as required. The slide-in unit attaches to the F-ASP structure immediately after the primary pickoff and before the system calorimeter of the beam in which it is installed.

The DPR aids beam smoothing by splitting the light wave into its two component parts, the extraordinary (*e*) and ordinary (*o*) waves, so that when combined with a DPP, the intensity values of the beam become more evenly distributed (Fig. 5.9-3). By driving the high-intensity values toward the mean intensity, a reduction in speckle contrast is obtained. The KDP is oriented so that the vertex is halfway between the orthogonal extraordinary and ordinary axes. The *e* and *o* waves are oriented in an orthogonal direction with respect to one another, and they travel at different speeds due to their different indices of refraction through the crystal. This speed difference is necessary because it produces a phase shift that prohibits formation of interference fringes that would be detrimental to the beam-smoothing effect. As the *e* and *o* waves leave the DPR, they are orthogonally polarized and angularly separated by about 80 μm on target. When the beam is viewed just prior to entering the chamber with the DPP alone, there are many high intensities, or "hot spots," in it. This speckle pattern is produced by the DPP. When the DPR is optimally aligned, it reduces this speckle, and therefore the contrast of the beam, by a factor of $\sqrt{2}$ to yield a more-uniform illumination.

Table 5.9-1
Opposing Beam Pairs on the
OMEGA Target Chamber

Beam			Beam			Beam			Beam	
1	1	⇔	5	4		4	1	⇔	1	8
1	2	⇔	5	5		4	2	⇔	3	7
1	3	⇔	4	3		4	3	⇔	1	3
1	4	⇔	4	8		4	4	⇔	1	0
1	5	⇔	5	3		4	5	⇔	1	7
1	6	⇔	4	7		4	6	⇔	2	5
1	7	⇔	4	5		4	7	⇔	1	6
1	8	⇔	4	1		4	8	⇔	1	4
1	9	⇔	5	6		4	9	⇔	2	4
1	0	⇔	4	4		4	0	⇔	3	5
2	1	⇔	5	8		5	1	⇔	2	0
2	2	⇔	6	4		5	2	⇔	2	3
2	3	⇔	5	2		5	3	⇔	1	5
2	4	⇔	4	9		5	4	⇔	1	1
2	5	⇔	4	6		5	5	⇔	1	2
2	6	⇔	5	0		5	6	⇔	1	9
2	7	⇔	6	0		5	7	⇔	2	8
2	8	⇔	5	7		5	8	⇔	2	1
2	9	⇔	6	8		5	9	⇔	3	4
2	0	⇔	5	1		5	0	⇔	2	6
3	1	⇔	6	2		6	1	⇔	3	0
3	2	⇔	6	3		6	2	⇔	3	1
3	3	⇔	6	9		6	3	⇔	3	2
3	4	⇔	5	9		6	4	⇔	2	2
3	5	⇔	4	0		6	5	⇔	3	9
3	6	⇔	6	7		6	6	⇔	3	8
3	7	⇔	4	2		6	7	⇔	3	6
3	8	⇔	6	6		6	8	⇔	2	9
3	9	⇔	6	5		6	9	⇔	3	3
3	0	⇔	6	1		6	0	⇔	2	7

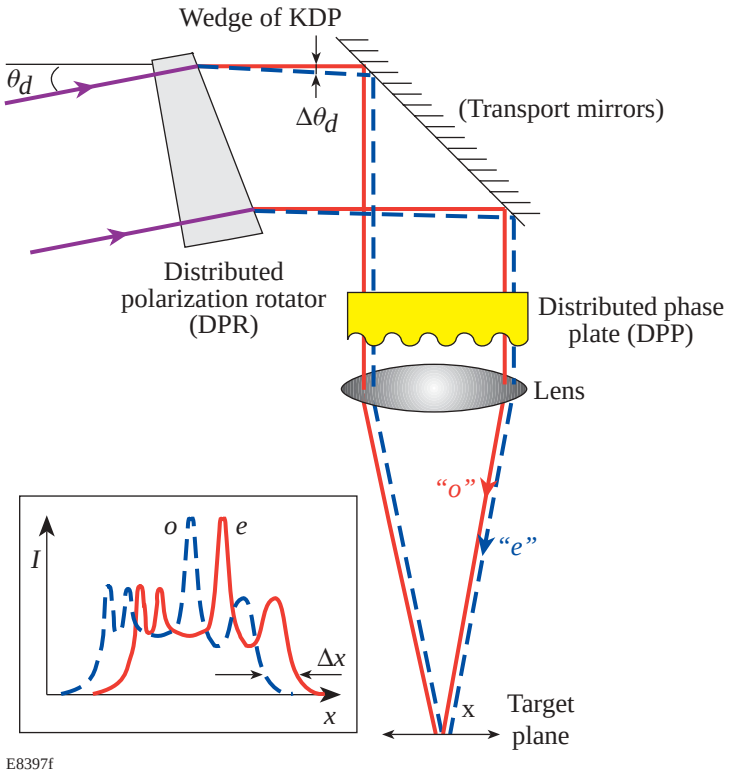

Figure 5.9-3
A distributed polarization rotator and a distributed phase plate work together to increase the target plane irradiance uniformity.

Transport Mirrors

The 120 end mirrors and target mirrors are used at angles of incidence ranging from 45° to 60° and have a sufficient unobstructed aperture to handle the 280-mm-diam, high-power UV beams. There are three sizes of transport mirrors, all elliptical in cross section and fabricated from Pyrex™ substrate material: 14 in. × 20 in. × 2 in., 14 in. × 27 in. × 3 in., and 14 in. × 27 in. × 2 in. The mirrors are coated for high reflectance (≥99.5%) at 351 nm and have damage thresholds ≥2.8 J/cm^2. The frequency-converted beams incident upon the end mirrors still contain up to 30% residual 1053-nm and 527-nm energy. Since the end-mirror coating reflects only the 351-nm light, the residual red and green energy passes through the front surface coating and the mirror substrate and is scattered by a shield located between the mirror substrate and the mount. This process ensures that only 351-nm energy reaches the target chamber.

An additional optical feature on most of the end and target mirrors is a 2-in.-diam piece of 1053-nm absorbing glass (Schott KG3) that is glued to the back of the mirror near the center. This glass is index matched to the Pyrex™ substrate to absorb a small-diameter, 1053-nm beam from the IRAT that passes through the front-surface coating during the beam-timing process. Since the HR @ 351-nm coating on the front surface reflects only ~0.5% @ 1053 nm, the 4% reflection from the back surface could compete with the signal from the front-surface reflection. The design features of the beam-timing system are more fully described in Chap. 6.

The transport mirrors are each mounted in the dual-plate, single-pivot-type mount shown in Fig. 5.9-4. Flexures and high-resolution, dc-motor-driven actuators provide angular adjustment. Since the transport mirrors are oriented at almost every angle with respect to gravity (except exactly vertical or horizontal), the mount is designed with several variations. The mount is also designed to fit in a limited-space envelope because of the congestion of beams in the target area. The two 1-in.-thick steel plates are held together by, and pivot about, a single flexure. The two actuators are located such that they form a right angle about the pivot bearing and are spring loaded by three rod flexures that also connect the two plates. This combination of flexures, actuators, and a flexure pivot provide for orthogonal tip and tilt of the mirror with 1-μrad pointing resolution over a range of ±0.25°. Analysis of the design shows that the pivot/flexure mount design has pointing drift stability of ≤3 μrad over 30 min at 70°F. Several different sets of flexures with varying stiffness keep similar loads on the actuators at the different orientation angles with respect to gravity.

The transport mirror mounts are designed to preserve a mirror surface figure of ≤100 nm peak-to-valley at any angle with respect to gravity. To accomplish this, the mirrors are supported on two edge-support pads and held down with three surface pads. The mounts are always oriented to locate the two edge-support pads downward, so that the mirror's elliptical edge rests on them. The mirror pad/clamp assembly is reversible in configuration depending on the orientation of the mirror surface to gravity. A hard pad on a ball-bearing pivot supports the mirror (front or back surface) from the downward side and provides a stable reference for angular stability. A rubber pad then bears upon the mirror's opposite (upper) surface and is clamped tight enough to keep the mirror from moving, without distorting the optical figure. To preserve the mirror figure at each angle with respect to gravity, the three-point edge mount is augmented by a fourth center support—a 1.5-in. round pad epoxied to the back of the mirror. A rod and spring combination is used to provide a push or pull force on the center pad. Prior to final installation the spring force (precalculated for each mirror orientation) is tuned while the mirror is under interferometric test at its installed angle with respect to gravity.

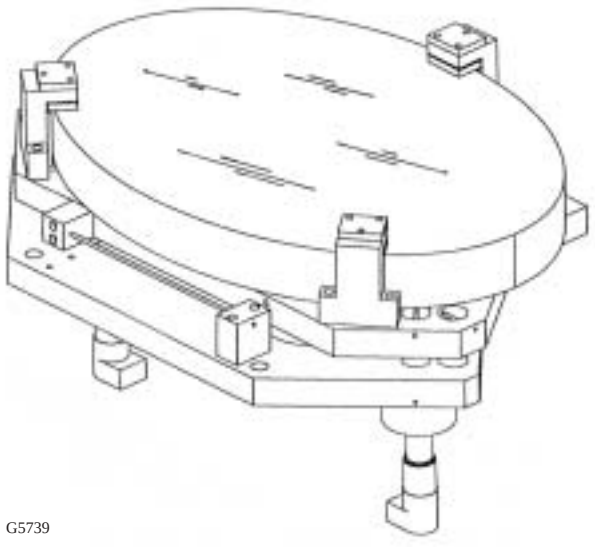

Figure 5.9-4
The mirror mount consists of two plates and four flexures.

The end mirrors are mounted on the end-mirror structure at their design angle. Each location on the structure has a painted steel mounting surface oriented parallel to the mirror surface to which the mount is bolted for coarse angular setting. The mount plate is one of a set of welded angle plates (customized for each mount location) that provide the proper angular interface and standoff distance from the structure. The target mirror mounts are held inside interface structures mounted on the ends of the 60 hexagonal tubes of the TMS. These small structures consist of a welded steel box, which contains the mirror mount, welded to a standoff tube that is bolted to the TMS hex tube. Each standoff is cut at the proper angle to the structure to set the mirror mount to receive the incoming beam and reflect it down the axis of the hex tube (see Fig. 5.2-5).

Focus Lens Assembly (FLAS)

The FLAS is the optomechanical assembly that mounts and positions the focus lens and provides for mounting the blast/vacuum window and debris shield on the target chamber. The optomechanical requirements for the FLAS were determined from the optical design and the pointing error budget and are shown in Table 5.9-2.

The focus lens has a focal length of 1.8 m and functions at *f*/6 (300-mm c.a.). The lens and the blast window, a 325-mm-diam × 25.4-mm-thick plano optic, produce less than a quarter wave of aberration (at 351 nm) over a field of view (FOV) of ±2 mm. The debris shield, a disposable 297-mm-diam × 5-mm-thick plano optic that serves as the primary source of protection from target debris, is also designed to produce less than a quarter wave of aberration. The FLAS design provides a location, just ahead of the lens, for a DPP (distributed phase plate), which is a plane-parallel, fused-silica component 310 mm in diameter and 14 mm thick. The optical design also ensures that damage-causing ghost reflections do not fall on any optics for any focus lens position (over a range of ±10 mm).

Table 5.9-2
Summary of Requirements for Focus Lens Assembly

Centration of lens to port axis	0.25 mm
Maximum *static* tilt of lens	0.28 mrad
Blast-window thickness	25 mm
Focus range	10 mm
Maximum transverse motion (over focus range)	1.6 μm
Additional focal shift	+10 cm
Transverse vibration	<0.6 μm
Axial vibration	2.5 μm
Focus accuracy	25 μm
Surface deformation	<100 nm
Vacuum differential (supported by blast window)	760 Torr
Note: Positive motion is *away* from the chamber center.	

The optical requirements are met with an aspheric singlet lens, designed to be free of spherical aberration when used in conjunction with a 25.4-mm-thick blast window. The curvatures of the singlet were chosen to position the ghost reflections away from all optical components in the OMEGA beam transport optical system. This selection of curvatures somewhat compromised the attainable FOV, since the lens shape that would maximize FOV (i.e., minimize coma) would have caused potentially damaging ghost reflections to fall on nearby optics. Despite this compromise, the FOV provided by the final design is ±4.5 mm, significantly exceeding the original requirement.

The FLAS subsystem is shown in Fig. 5.9-5. The drawing on the left side of the figure depicts the entire assembly including the blast window removal mechanism. The drawing on the right side of the figure is a cutaway of the focus-lens barrels and shows the position of the focus lens and blast window.

The optomechanical design of the FLAS was driven primarily by the transverse motion tolerance of 1.6 μm over the 10-cm focus range. Previous experience with the 24-beam OMEGA focus lenses indicated that rolling bearings cannot provide this accuracy. The final design for the upgraded OMEGA system incorporates solid bearings consisting of polymer pads (i.e., Vespel™) running against polished steel ways. Analysis shows that this design provides sufficient stiffness and linearity of motion to satisfy the requirements.

To meet the centration requirements, as well as permit alignment of the focus axis to the center of the chamber, adjustments are provided on the bearing pads. Datum surfaces on the end of the lens barrel enable accurate location of the optical axis of the lens with respect to the axis of the focus motion on the mount, allowing alignment of both to the center of the chamber within tolerance.

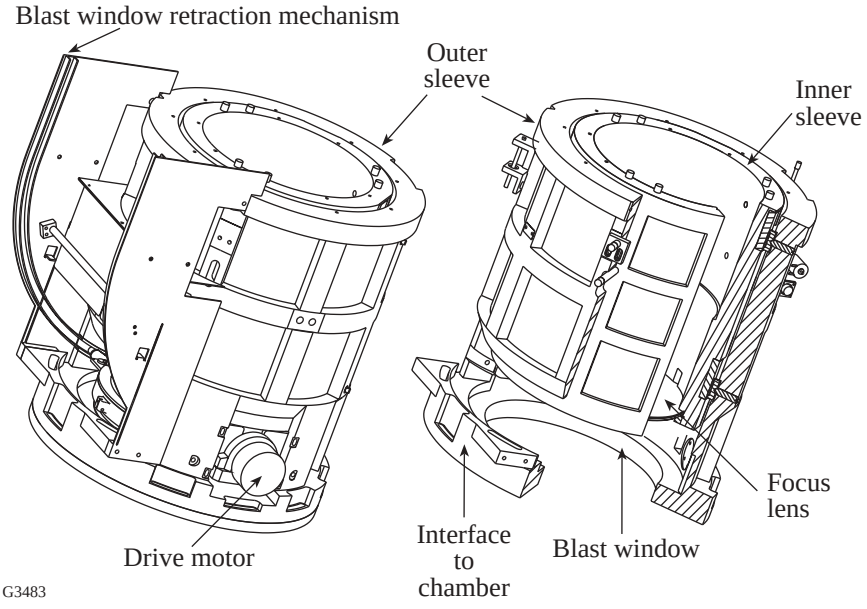

Figure 5.9-5
The FLAS for OMEGA. To the left is the entire assembly including the blast-window retraction mechanism. To the right is a section of the two sleeves showing the position of the focus lens and blast window.

One of the main challenges of the FLAS design was the additional requirement that the blast window assembly (BWA), consisting of the blast/vacuum window and debris shield, be removed frequently for service. The blast window is changed or cleaned on a regular basis as it becomes contaminated or damaged; the debris shield may be cleaned and recycled a number of times until it is eventually disposed of upon reaching a damage threshold. To achieve the necessary stiffness and pointing accuracy, the FLAS has to be fairly large; it nearly fills the space between the target chamber and the TMS. As a result, space constraints in the vicinity of the target chamber make it impossible for one to reach in and remove the BWA directly. A mechanism was designed to assist with this process. This rail-like mechanism transports the BWA from the target chamber to the exterior of the TMS, where it can be grasped and removed. The mechanism works in reverse to return the BWA from the outside face of the TMS to the target chamber, where it is correctly positioned and clamped to initiate the vacuum seal. That mechanism is shown in Fig. 5.9-5.

Distributed Phase Plates (DPP's)

The purpose of the DPP's is to smooth the intensity fluctuations that would normally be present in a focused, high-power laser beam. This results in a fine speckle pattern distributed over the full diameter of the target. When combined with SSD, the fine speckle pattern moves at high frequency (several GHz) during the time of the pulse, thus producing a smooth focal spot.

For efficient phase conversion of the high-power UV beams, continuous DPP's are used. These DPP's are deep-surface-relief, continuous phase plates that exhibit near-unity energy efficiency, envelope and power spectrum flexibility, and reduced near-field intensity modulation as compared to stepped diffractive optics as used on the 24-beam OMEGA. The DPP's are used to reduce high-intensity hot spots in the far field of the focused beams, and they are insensitive to near-field wavefront errors that have accumulated from the optical components in each beam. The continuous-phase DPP's can perform nearly lossless phase conversion of high-power laser beams, thus delivering up to 25% more laser energy to the fusion targets than with binary DPP's, and with much greater uniformity than with no DPP at all. They are designed specifically to provide the desired intensity envelope and speckle distribution over the range of 700- to 1000-μm target diameter. A more complete description of the DPP's can be found in Ref. 8.

The DPP's are 310-mm-diam. $\times$ 14-mm-thick flat fused-silica windows that have the DPP elements on one side. Both surfaces are AR coated at 351 nm. They are mounted to the inner sleeve of the FLAS, just ahead of the focus lens. This location is chosen to avoid any lethal ghost reflections from the focus lens and blast window. The DPP is also tilted by 6° to the optical axis to avoid producing any lethal ghosts within the optical train. The DPP mounts are manually installed (i.e., not flip-in devices); therefore, once they are in place, targets must be aligned through the DPP. Both image processing and maximization of the reflected energy signal from a surrogate target are used to point and focus the alignment beams on target through the DPP's.

$2\omega/4\omega$ Probe Beam

OMEGA has been modified to deliver one high-power beam to the Target Chamber Center at either 527 nm (visible green, also termed "2ω") or 263 nm (ultraviolet, also termed "4ω.)" This is achieved by tuning the FCC in beam 25 to optimize production of 2ω, intercepting the beam before it arrives at its end mirror and directing through a special, 61st FLAS on Target Chamber port P9. For 4ω operation, a KDP doubler is inserted into the beam path and the focus lens is changed.

The special FCC tuning involves detuning the triplers to preclude generation of the normal third harmonic ("3ω") and tuning the doubler crystal to optimize the output of the second harmonic. This allows approximately 400 J of green laser energy to be delivered to the target.

After being redirected by a removable, kinematically mounted, green beam end mirror, the beam is transported by two permanently mounted green beam transport mirrors to the target chamber (see Fig 5.9-6). The beam enters the target chamber through a focus lens assembly in port P9, specifically designed to operate at the green wavelength. The transport mirrors and green FLAS allow a pointing accuracy of 100 μm. The difference between the green beam path length and the nominal UV path length is resolved by the path length adjustment system, resulting in a timing accuracy of 100 ps.

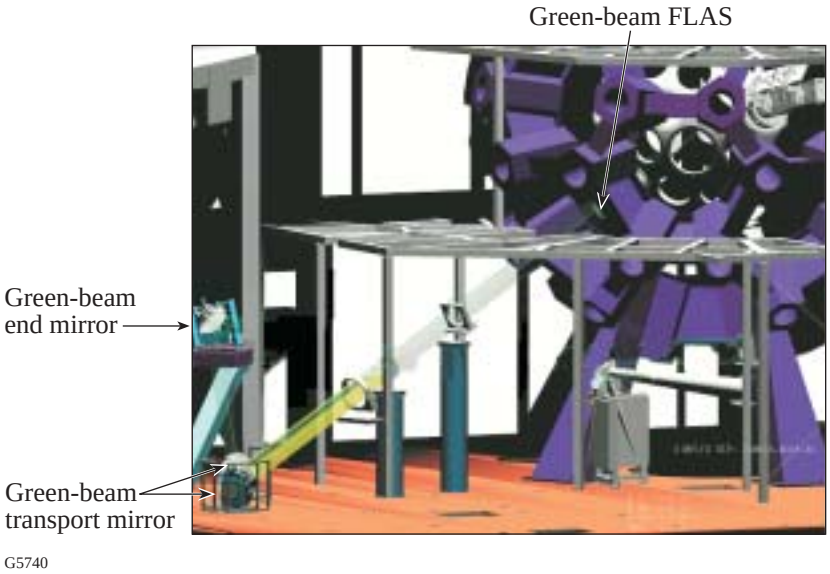

Figure 5.9-6
Green beam transport optics in the Target Bay.

Alignment of the green beam is accomplished with a green alignment laser arm located on the north side of the UVAT (see Fig 5.8-10). The diode-pumped laser and the flash-lamp-pumped laser both have 527-nm output capability. A simple flip-in mirror on the UVAT allows reconfiguration between the two lasers; the diode-pumped laser is the nominal source for green beam alignment. A green beam ASP senses the pointing of the reflected beam for targeting purposes.

Details of the 4ω sysem are still in development.

5.10 BEAMLINE CONTROLS

The controls for the alignment and beamline diagnostic subsystems integrate and monitor approximately 200 control points. While the primary control locations for system shots are the workstations-designated "bay" and "palm" in the Control Room, local control stations can be set up in the Laser Bay and Target Bay as required. General positioning, sensing, and switching tasks are handled by an LLE-developed system based on the Echelon^{10} local operating network (LON®) and Neuron® technologies. The LON® is based on a communication protocol known as LonTalk®, which is similar to, but in many ways more robust than, the more familiar TCP/IP (telecommunications protocol/Internet protocol). A LON channel consists of a number of control/communication "nodes" connected to a

medium such a cable or fiber-optic link. The OMEGA control system makes use of about two dozen individual LON channels, or LON's, arranged by physical layout and application. In each node, the facilities necessary to implement LonTalk® are provided on a chip-set that includes a single-chip multiprocessor known as a Neuron®. The Neuron® also provides memory and computing capabilities that can be programmed by users. Video cameras are used as alignment diagnostics throughout the system. These cameras and a limited set of surveillance cameras are linked together in a computer-controlled closed-circuit television (CCTV) system.

Figure 5.10-1 is a block diagram of the alignment computer controls. The beamline diagnostic configuration illustrated in Fig. 5.7-4 is also operated by the same workstations. The alignment configuration provides control and data acquisition for the beamline optics from the stage-A splitter through the focus lenses. The neuron module/LON devices in the Optomechanical System can be broken down into four classes, as defined by the type of actuators they have, and can control the module to which they interface. These classes are listed in Table 5.10-1. The alignment system uses the neuron daughter board and device-specific mother boards as building blocks. A neuron card cage is used to mount the neuron modules in each of the laser structures.

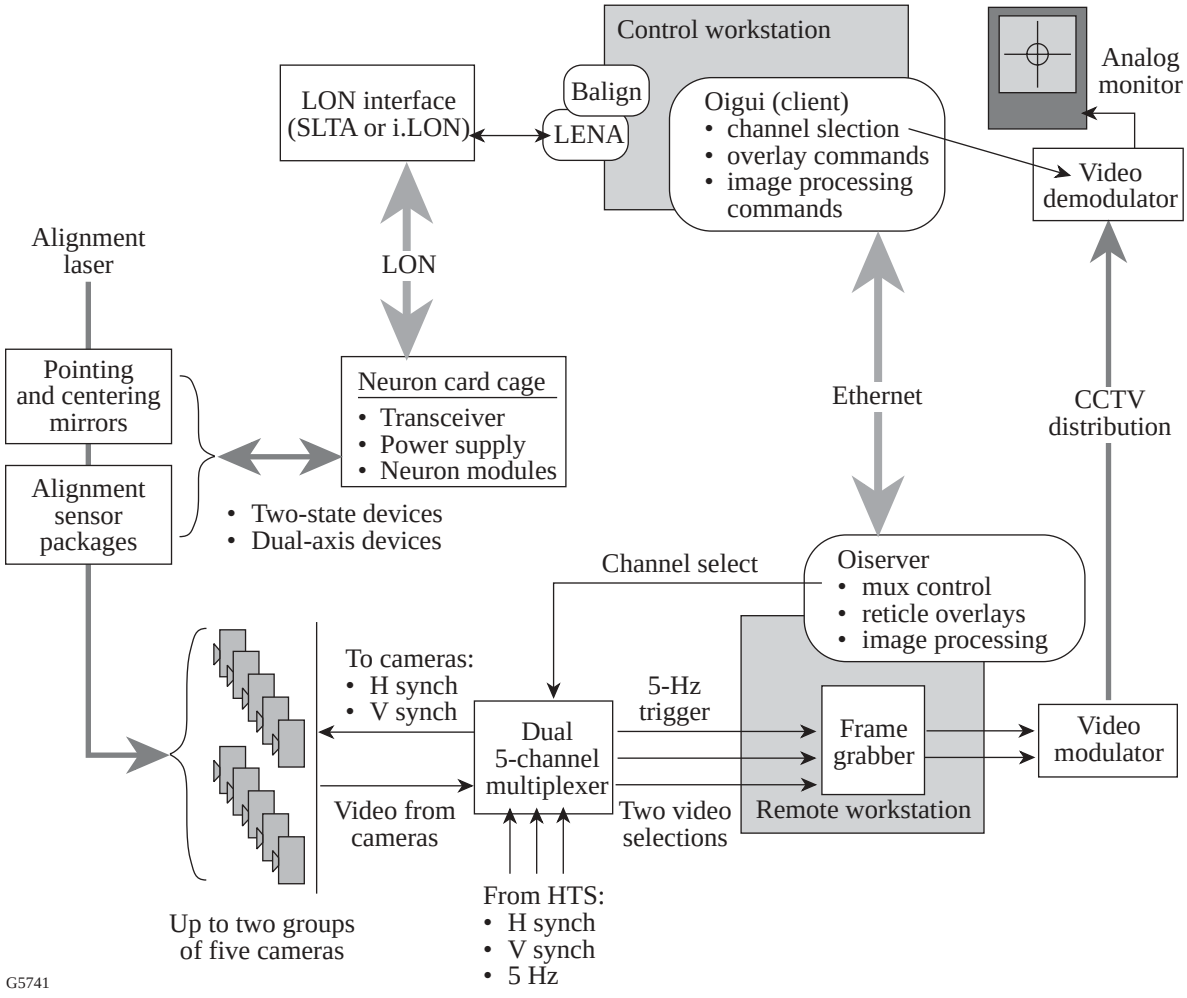

Figure 5.10-1
The alignment control configuration implements a loop closed at the executive level and other control and acquisition functions. Beamline diagnostics are supported by additional items interfaced to the same host processor.

Table 5.10-1
Alignment/Beamline Diagnostic
Device Control Classes

Device	Actuator	Control Module
4.5-in. × 6-in. mirror mount	dc motor and encoder	Dual axis – DACM
5.5-in. × 7-in. mirror mount	dc motor and encoder	Dual axis – DACM
transport mirror mount	dc motor and encoder	Dual axis – DACM
spatial filter manipulator	dc motor and encoder	Dual axis – DACM
frequency converter gimbal	dc motor and encoder	Dual axis – DACM
ASP focus	dc motor and encoder	Dual axis – DACM
rotating wave plate	dc motor and A/D converter	Single axis – SACM
path-length adjuster (PALS)	dc motor and A/D converter	Single axis – SACM
focus lens mount (FLAS)	dc motor and A/D converter	Single axis – SACM
shutters flip in	N_2 pneumatic	Two state – TSCM
cross-hairs flip in	N_2 pneumatic	Two state – TSCM
12-in. calorimeters flip in	N_2 pneumatic	Two state – TSCM
ASP flip-in optics	N_2 pneumatic	Two state – TSCM
calorimeter data acquisition	—	Generic A/D – GADM
spatial filter vacuum riser sense and control	A/D converter and DC motor converter	Generic A/D – GADM
FCC crystal temperature	A/D converter precision	Generic A/D – GADM

Neuron Modules (Generic)

The alignment system's mother-board/daughter-board concept is shown in Fig. 5.10-2. The basic daughter boards and the device-specific mother boards are physically and electrically integrated to become a neuron module (NM) that fits into a neuron card cage. The mother board receives power and LON network communications from the card cage and has local control and device control connectors on its front face. Separate mother-board designs are used for each of the control device classes:

- two-state device control module (TSCM),
- dual-axis control module (DACM),
- single-axis control module (SACM), and
- generic analog/digital converter module.

A unique code wired into each type of mother board allows the neuron to determine which application program should be loaded into its application image space.

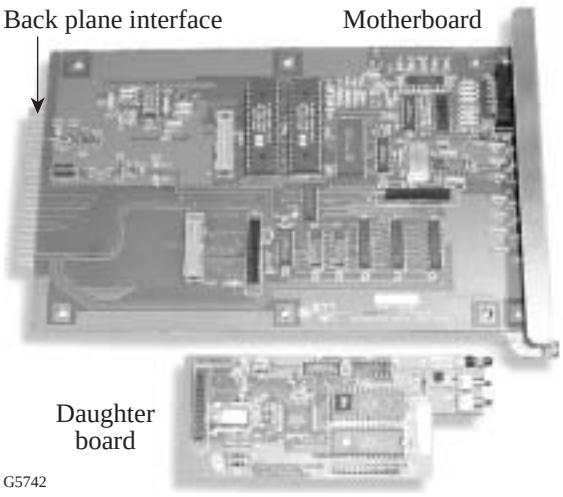

Figure 5.10-2
Mother-board/daughter-board concept.

Neuron Card Cage

The neuron card cage (shown in Fig. 5.10-3) is a rugged enclosure designed to mount in a standard 19-in. panel rack at the base of each laser structure. It has provisions for 12 insertable modules: a power supply, a LON transceiver, and ten neuron-based device control modules. The card-cage power supply converts facility 110 VAC power to the ±12 VDC and ±5 VDC sources that are needed by the other card-cage modules. The card-cage back plane incorporates connectors and circuit traces that distribute power and signals to the 12 modules, allowing them to be inserted and removed from the front of the cage.

The external cables for power, communication, and connection of the device control modules to the laser system devices run under the cage from the back and connect to the front of the modules. This combination of front-panel and back-plane connections allows for rapid removal and replacement of a failed or suspect module.

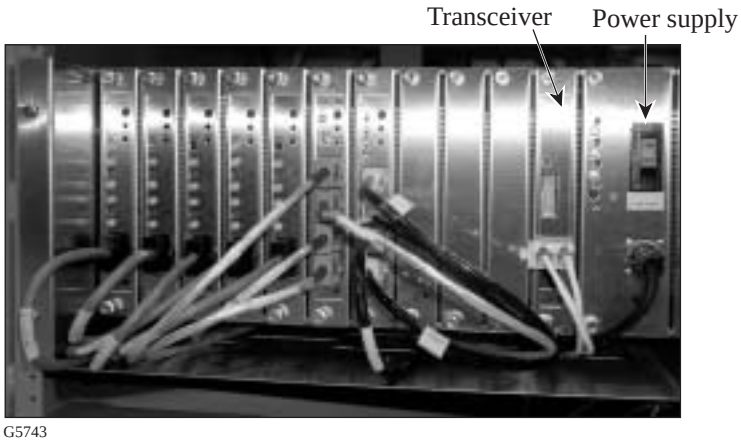

Figure 5.10-3
Neuron card-cage concept.

Transceiver and Back Plane

The basic function of the transceiver is to electrically match a twisted-pair LON medium to the printed circuit LON extension that is built into the back plane. The result is that while each of up to ten neurons in the card cage can function as an independent node in the context of the LONTalk protocol, the entire cage is a single "load" in the electrical signal context.

The transceiver also incorporates three rotary switches that are set to provide a card-cage identifier that can be accessed by the neurons via the back plane. The back-plane circuit traces also provide a cage slot identifier to each neuron. These features allow each neuron node to "know" its own unique location on the LON channel.

Individual Device Controllers

The three types of NM's defined to meet the needs of the optomechanical devices for alignment and laser operations are as follows:

Two-State Control Module (TSCM): The alignment system includes hundreds of devices that are either on or off, in or out. The TSCM mother board allows the associated neuron daughter board to control four of these devices independently. Each of the four "channels" provides the following services at the front connectors:

- a pair of firmware-controlled switch closures (1.5 A, 60 VDC max),
- fused +12 VDC (50 mA max),
- +5 VDC,
- inputs for two optional device-mounted limit switches, and
- appropriate grounds.

The electrical and pneumatic control connections for a typical flip-in device are shown in Fig. 5.10-4.

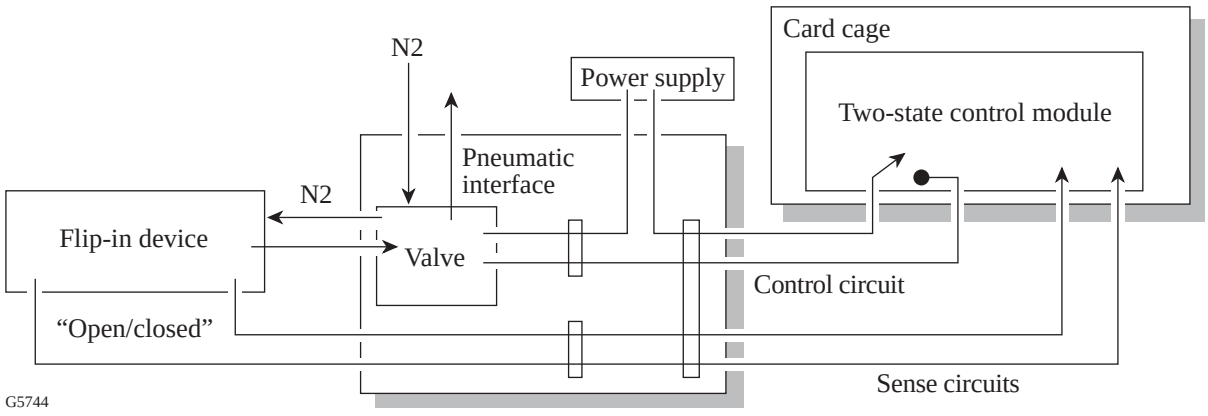

Figure 5.10-4
Flip-in devices control and sense connections for a single device channel. The power supply and pneumatic interface assemblies can support a number of device channels in an optomechanical structure.

The application firmware is capable of

- closing/opening the switch contacts in response to commands from the executive process,
- using the limit switch inputs to determine the status of the device, and
- transmitting success/error messages back to the executive process.

Dual-Axis Control Module (DACM): The DACM is typically used to position mirrors or spatial-filter pinholes. The dual-axis controller mother board allows the associated neuron daughter board to control two servo motors independently. Each of the "channels" provides the following services at the front connectors:

- firmware switched ±12 VDC (100 mA max) for servo motor drive,
- quadrature motor shaft encoder inputs,
- inputs for two device-mounted limit switches, and
- appropriate grounds

The application firmware is capable of moving the motor shaft a specified number of encoder steps in either direction in response to commands from the executive process. To avoid backlash, a programmable overshoot and return function allows each move to be completed from the same direction. The shaft encoder inputs are also used to determine the status of the device. The limit switch inputs are used to avoid driving into the device's hard stops. Success/error messages are transmitted back to the executive process.

Single-Axis Controller (SACM): The SACM is typically used to position rotating wave-plate polarizers. The mother board allows the associated neuron daughter board to control a servo motor and receive digitized absolute-position feedback data. The mother board provides the following services at the front connectors:

- firmware switched ±12 VDC (100 mA max) for servo motor drive,
- input to an analog-to-digital (A/D) converter suitable for use with a linear potentiometer, and
- appropriate grounds.

The application firmware is capable of moving the motor shaft to achieve a specified encoder position using a feedback control algorithm in response to commands from the executive process. To avoid backlash, a programmable overshoot and return function allows each move to be completed from the same direction. The position sensor inputs are also used to determine the status of the device. Success/error messages are transmitted back to the executive process.

LON Channels

Figure 5.10-5 illustrates the Laser Bay and Target Bay areas that are controlled by the eight alignment LON channels. In general, each channel has card cages that contain modules of all types. The layout was established by balancing LON cable length and transceiver load guidelines for good signal performance against the physical locations of the devices to be controlled. An additional LON channel, AT-9, serves the 12-in. calorimeters at the F-ASP's.

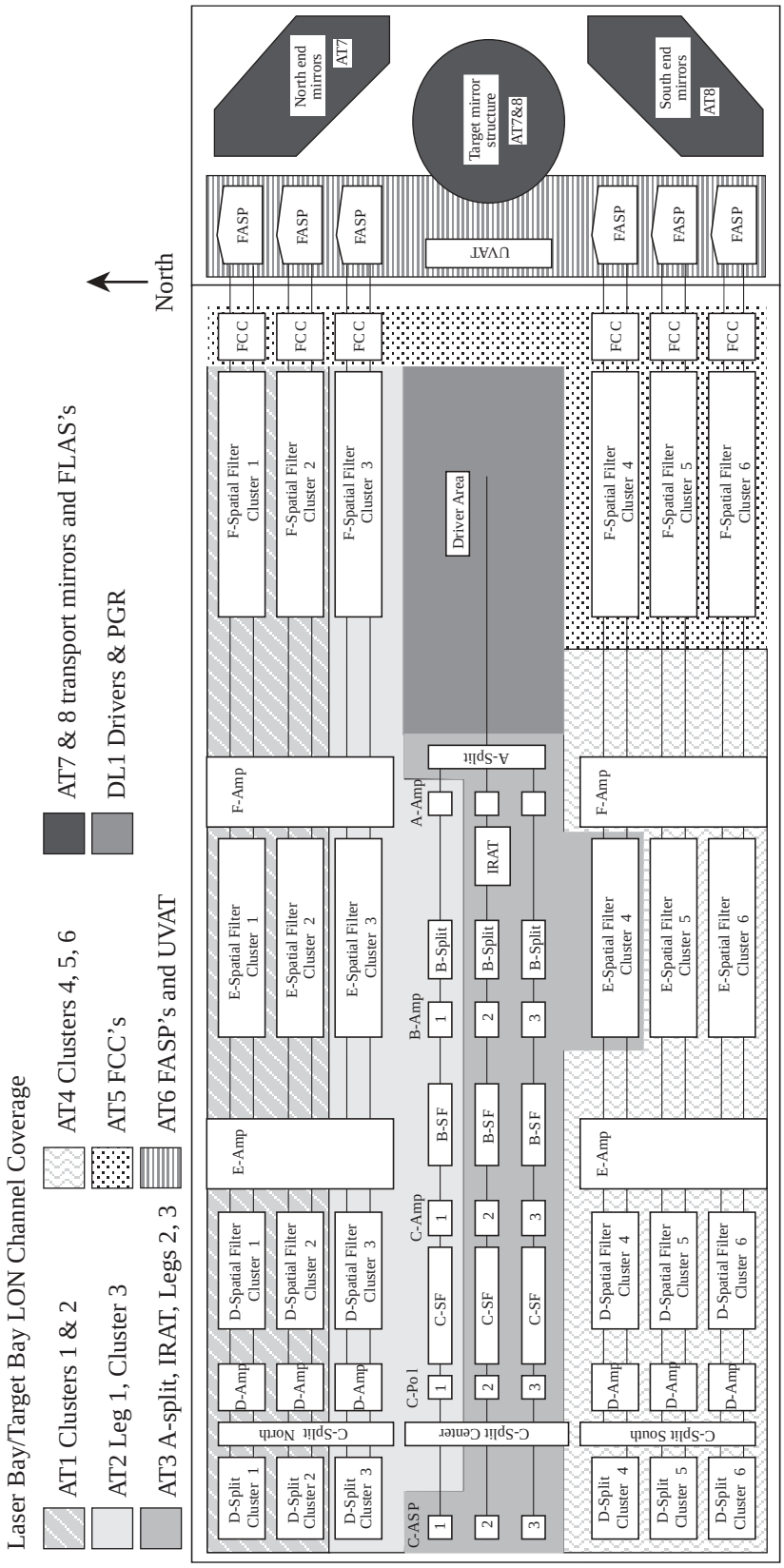

Figure 5.10-5
Laser Bay/Target Bay LON channels.

Alignment Loop Implementation

Figure 5.10-1 illustrates the basic control elements that are used for in-beam alignment. The operator uses a Sun workstation (top center) to control the system and views the results on an analog video monitor. Operator stations of this type are provided in the Control Room, the Laser Bay, and the Target Bay. This arrangement is applicable to pointing or centering in either the IR or the UV portions of the system and to pinhole centering. Other optomechanical activities make use of similar configurations

An application program called ***balign*** provides a graphical interface that allows the operator to control the optomechanical devices in the beam train and displays information about their status. As shown on the left in Fig. 5.10-1, the operator uses ***balign*** to control the beam train and the associated alignment sensors. The command and status communication is implemented by a ***lena*** (LON/Ethernet network adaptor) application program. In the current implementation, the ***lena*** communicates with a separate Serial LONTalk Adaptor (SLTA) connected to the SUN workstation via an RS-232 link. Each SLTA supports a single LON, and SLTA's for each of the LON's shown in Fig. 5.10-5 are located in a cabinet in the Control Room. LON cables extend from there to the neuron card cages in the Laser Bay and Target Bay. In the near future, the SLTA's will be replaced by "i.LON" units, which will be connected to the SUN workstation by the Ethernet LAN.

The results of the operator's actions are interpreted from the images acquired by the CCD cameras in the alignment sensor packages (ASP's). The figure shows two groups of five cameras, which is typical of the configuration that supports one cluster of beams at the F-ASP. An LLE-designed, dual, five-channel multiplexer is used to provide synchronization signals derived from the Hardware Timing System to the cameras. The multiplexer selects the signal from one camera in each group of five and connects it to a frame grabber that is installed in a Sun workstation located in the bay near the ASP. Depending on its other uses, each of these remote workstations can host up to three multiplexer/ frame grabber setups. The multiplexer is connected to the Sun workstation via an RS-232 link.

The frame grabber provides analog video outputs that are connected to the closed-circuit television system. These outputs can be "live" raw images; near-real-time, sequentially processed images; or single, frozen frames. The operator uses an application program called ***oigui***, which run the control workstation, to connect to an ***oiserver*** program on the remote workstation and control the selection and processing of the video images. The server can grab, image, and perform any of several standard analyses on the video data. The results can be displayed graphically on the video image by making use of an overlay feature of the frame grabber. This feature is also used to display reticles on the video images.

The ***oiserver/oigui*** system functions to coordinate the input and processing actions of the remote computer with the CCTV channels displayed on the local monitor. This is facilitated by a commercial serial-controlled video demodulator unit connected to the control station computer via an RS-232 link. The images are interpreted as a deviation from the desired value. If an adjustment of the optical train is necessary, commands are passed to the appropriate DACM's. Pointing and centering alignment generally involves commands to two DACM's, one that positions a pointing mirror and one that positions a centering mirror. The pinholes in spatial filters are positioned by a single DACM.

Note that these alignment "control loops" are closed stepwise (measure, compute, move, measure) over a period of 10 s to about 1 min; these are not real-time loops.

5.11 REFERENCES

1. R. S. Craxton, ed., *OMEGA Upgrade Preliminary Design*, Laboratory for Laser Energetics, Report DOE/DP 40200-101, University of Rochester (1989).

2. *Optics Coating Requirements Document, OMEGA Upgrade No. M-AA-G-05, Rev. A*, Laboratory for Laser Energetics, University of Rochester, Rochester, NY (1992).

3. "Development of Optical Coatings for the OMEGA Upgrade," Laboratory for Laser Energetics LLE Review **44**, 219–232, NTIS document No. DOE/DP/40200-140 (1990). Copies may be obtained from the National Technical Information Service, Springfield, VA 22161.

4. "High-Reflectance Transport-Mirror Development for the OMEGA Upgrade," Laboratory for Laser Energetics LLE Review **51**, 139–155, NTIS document No. DOE/DP/40200-204 (1992). Copies may be obtained from the National Technical Information Service, Springfield, VA 22161.

5. *Optical Coating Specification Document, OMEGA Upgrade No. M-AA-G-07*, Laboratory for Laser Energetics, University of Rochester, Rochester, NY (1993).

6. R. S. Craxton, "High Efficiency Frequency Tripling Schemes for High Power Nd:Glass Lasers," IEEE J. Quantum Electron. **QE-17**, 1771–1782 (1981).

7. R. S. Craxton, ed., *OMEGA Upgrade Preliminary Design*, Laboratory for Laser Energetics, Report DOE/DP 40200-101, University of Rochester (1989).

8. M. A. Henesian, C. D. Swift, and J. R. Murray, "Stimulated Rotational Raman Scattering in Nitrogen in Long Air Paths," Opt. Lett. **10** (11), 565–567 (1985).

9. T. J. Kessler, Y. Lin, J. J. Armstrong, and B. Velazquez, "Phase Conversion of Lasers with Low-Loss Distributed Phase Plates," in *Laser Coherence Control: Technology and Applications*, edited by H. T. Powell and T. J. Kessler (SPIE, Bellingham, WA, 1993), Vol. 1870, pp. 95–104.

10. Echelon Corporation, San Jose, CA 95126. (Echelon LON™, Neuron™, LONtalk™, and i.LON™ are trademarks of Echleon Corporation.)